CONTRIBUTION OF HIGH HISTONE ACETYLATION IN MEMORY ALLOCATION

ANA BEATRIZ REIS DOS SANTOS MARQUES

A dissertation submitted in partial fulfillment of the requirements for the Degree of Masters in Biomedical Research (Specialization Area: Neuroscience) at Faculdade de Ciências Médicas | NOVA Medical School of NOVA University Lisbon

January, 2022

CONTRIBUTION OF HIGH HISTONE ACETYLATION IN MEMORY ALLOCATION

Ana Beatriz Reis dos Santos Marques
Supervisors: Prof. Johannes Gräff, Associate Professor, Principal Investigator,
at Swiss Federal Institute of Technology Lausanne (EPFL), Lausanne, Switzerland,
and Prof. Rita Teodoro, Associate Professor, Principal Investigator,
at NOVA Medical School of NOVA University of Lisbon, Lisbon, Portugal

A dissertation submitted in partial fulfillment of the requirements for the Degree of Masters in Biomedical Research (Specialization Area: Neuroscience)

January, 2022

Acknowledgments

I would like to express my gratitude to everyone that, in one way or another, helped me throughout this year. Turns out the pandemic was still around and writing a Master's Thesis was more challenging than I imagined. But I am incredibly thankful for all the support that made this experience incredibly worthy.

To Prof. Johannes Gräff, for the amazing opportunity to conduct my Dissertation within his Laboratory at EPFL. For integrating me in the projects with great trust and for all the valuable insights.

To my supervisor, Giulia Santoni, a very special thank you for the trust, guidance and advice during all the Project. From technical skills to helpful feedback, all were of great help to reach this milestone. I am sincerely grateful for the growth experience, and the thoughtful advice that I will certainly carry with me.

To my supervisor and teacher, Prof. Rita Teodoro, for accompanying me throughout all my degree. For contributing to my growing passion for Neuroscience, for the continuous help, and for being a reference of a brilliant teacher and neuroscientist.

To the BIOP team, I would like to show my appreciation for the microscopy advice and script design that made the analysis of thousands of neurons, a lot easier.

To all the members of the lab, for being so welcoming and always ready to answer my questions. The lunch breaks, smiles in the morning, and cakes in the coffee room were truly a treat.

To the lab members and now friends, Lisa and Verena, for extending the laboratory hours to dinners and interesting conversations. They enriched this experience by offering all the help even in off work hours.

To my friends, who always encouraged and believed in me. Even at 2000 km away, they were always present and I am incredibly lucky for sharing this journey with all of them.

To my partner and his family, for showing me that Switzerland is more than delicious chocolate. From beautiful mountain views, the attempts to understand my messy French, and the unbelievable support, I am very thankful for feeling so at home during my stay.

To my family, I must express my immense gratitude for their unconditional support, for giving me the opportunity to study abroad, and specially for always being there, every step of the way. I would not be where I am without them.

Abstract

The process that defines how information is allocated in the brain is essential for the efficient storage and recall of a memory. At the time of encoding, neurons compete with one another to allocate a memory within neuronal populations. Interestingly, studies show that the number of cells recruited to the memory trace (or engram) is constant, and specific postsynaptic features define which neurons engage in memory storage. However, the mechanism that determines how neurons acquire such profile, eligible to became part of the engram, is poorly understood.

In the present study, we tested the contribution of histone acetylation, one of the most studied epigenetic mechanisms in learning and memory processes. By providing a chromatin conformation more permissive for gene expression, higher acetylation in histones bias the selection of neurons during memory encoding. Specifically, we examined two histone acetyl transferases (HATs), CBP and KAT5, as epigenetic signatures that mediate the allocation of a fear engram. Our results reveal that neurons with virally encoded HATs in the lateral amygdala (LA) are recruited to represent a fear memory, without altering the size of the engram. Conversely, increase in histone deacetylase 2 (HDAC2), in the same brain region, destabilizes the number of engram cells engaged, disturbing learning of the fear event.

These findings indicate that, to maintain a stable engram, neurons with higher HATs content in the LA are preferentially selected to represent a fear memory, whereas an acetylation imbalance by HDAC2-overexpression disrupts the competition for memory allocation. Unravelling the role of these groups of enzymes as upstream regulators of memory formation will contribute to the development of new therapeutic targets for memory-impairment conditions.

Keywords: engram size; neuronal competition; memory allocation; histone acetylation

Resumo

O processo que define de que forma informação é alocada no cérebro é essencial para o eficiente armazenamento e recuperação de uma memória. Durante a codificação de uma memória, neurónios competem entre si pela alocação de informação em populações neuronais. Curiosamente, estudos mostram que o número de células recrutadas para o traço de uma memória (ou engrama) é constante, e características específicas pós-sinápticas definem que neurónios são recrutados para o armazenamento da memória. No entanto, o mecanismo que determina de que forma os neurónios adquirem este perfil, tornando-os elegíveis para fazer parte do engrama, é pouco compreendido.

No presente estudo, testámos a contribuição da acetilação de histonas, um dos mecanismos epigenéticos mais estudados nos processos de aprendizagem e memória. Ao disponibilizar uma conformação da cromatina mais permissiva para a expressão génica, o aumento dos níveis de acetilação em histonas influencia a seleção de neurónios durante a codificação de uma memória. Mais especificamente, examinámos duas histonas acetiltransferases (HATs), CBP e KAT5, como características epigenéticas que medeiam a alocação de um engrama associado a medo. Os nossos resultados revelam que neurónios que codificam a forma viral de HATs no núcleo lateral da amígdala são recrutados para representar uma memória de medo, sem alterar o tamanho do engrama. Por outro lado, o aumento da histona deacetilase 2 (HDAC2), na mesma região do cérebro, destabiliza o número de células engrama, prevenindo a aprendizagem do evento de medo.

Estes dados indicam que, para manter um engrama estável, neurónios com elevado conteúdo de HATs na amígdala lateral são preferencialmente selecionados para uma memória de medo, enquanto que um desequilíbrio dos níveis de acetilação pela expressão de HDAC2 previne a competição pela alocação de uma memória. Desvendar o papel destes grupos de enzimas como reguladores da formação de uma memória contribuirá para o desenvolvimento de novos alvos terapêuticos para condições de comprometimento da memória.

Palavras-chave: engrama; competição neuronal; alocação de memória; acetilação de histonas

Funding

The project entitled ”Contribution of high histone acetylation in memory allocation” was developed at the Neuroepigenetics Laboratory and was supported by *École Polytechnique Fédérale de Lausanne* (EPFL) through funds from the grant StG 678832.

Contents

List of Tables

List of Figures

List of Abbreviations

Ac	Acetyl
Acetyl-CoA	Acetyl Coenzyme A
AD	Alzheimer's Disease
aFC	Auditory Fear Conditioning
APP	Amyloid Precursor Protein
Arc	Activity Regulated Cytoskeleton-associated protein
BSA	Bovine Serum Albumin
CamKIIα	Ca^{2+}/Calmodulin-dependent Protein Kinase II alpha
cAMP	Cyclic Adenosine 3,5-Monophosphate
CBP	CREB-Binding Protein
CRE	cAMP Response Element
CREB	CRE-Binding Protein
CS	Conditional Stimulus
CTX	Context
dB	Decibel
DNA	Deoxyribonucleic acid
eGFP	Enhanced Green Fluorescent Protein
H3K27ac	Histone 3 lysine 27 acetylation
HAT	Histone Acetyl Transferase
HC	Home Cage
HDAC2	Histone Deacetylase 2
IEG	Immediate-Early Gene
LA	Lateral Amygdala
LTP	Long-Term Potentiation
LV	Lentivirus
mA	(milli)Ampere

MAPK	Mitogen-Activated Protein Kinase
mg	(milli)Grams
mL	(milli)Liter
ns	Not Significant
PBS	Phosphate-Buffered Saline
PFA	Paraformaldehyde
PKA	Protein Kinase A
PTM	Post-Translational Modification
RNA	Ribonucleic Acid
RTS	Rubinstein-Taybi Syndrome
s.e.m	Standard Error of the Mean
TF	Transcription Factor
US	Unconditional Stimulus

Introduction

Our senses continuously collect information from the environment. The ability to retain that information is the basis of memory formation. Memories provide a link between past experiences and present behaviours, adapting our responses to environmental changes, accordingly.

To orchestrate such a complex process, sensory stimuli are perceived and processed in the brain through patterns of neuronal activity [1]. Ramón y Cajal was among the first to attribute the changes in the brain, after a memory is formed, at the level of single neurons [2] [3]. Neurons are specialized non-dividing cells that must remain highly adaptable to receive input from the environment. Simultaneously, neurons have to be reliable at processing, and storing information stably. The storage of information relies on the connectivity of populations of neurons so called neuronal ensembles [4]. As proposed by Donald Hebb, these are groups of neurons with coordinated firing activity that encode a memory [5] [6].

Decades later, these influential ideas were confirmed by empirical studies, providing insight on the mechanisms that sustain memory storage. The fundamental view in neuroscience agrees that memory formation involves strengthening of the synaptic connections between neurons [7]. Synapses are the structures that allow neurons to transmit information between each other through electrical or chemical signals, triggered by the activation of the presynaptic neuron [8]. Release of neurotransmitters from the presynaptic cell to the postsynaptic membrane of another are the basis of this communication (Figure 1.1) [9] [10]. Long-term potentiation (LTP), a persistent stimulation of the presynaptic neuron, triggers responses in the postsynaptic cell that lead to long-lasting increase in signal transmission between neurons [11] [12]. Consequently, formation of neuronal ensembles increases the likelihood that the same pattern of neuronal activity during a learning event, is repeated during its recall [7].

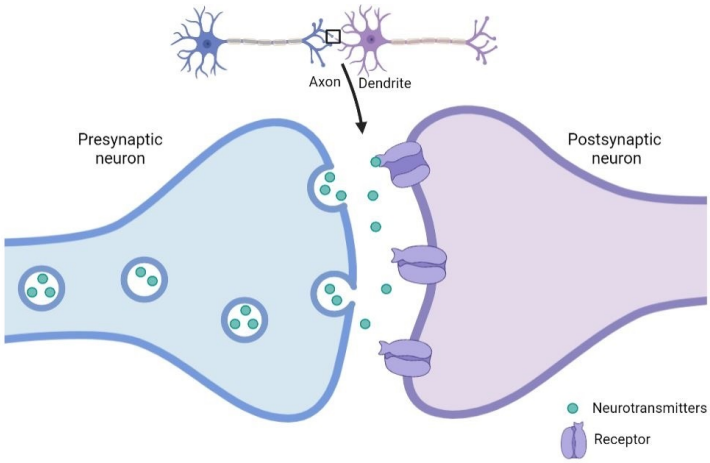

Figure 1.1: Chemical synapse. Chemical transmission between two neurons requires a sophisticated molecular machinery that regulates the release of neurotransmitters upon activation of the presynaptic terminal. The presence of postsynaptic receptors cable of detecting and translating the presynaptic message leads to postsynaptic events including synaptic remodeling.

1.1 Study of the memory process: finding the engram

The study of the cellular and molecular biology that accompanies memory storage was challenged by the inaccessibility of the brain, and the abundant number of cells that compose it. A more reductionist approach tried to overcome these challenges using invertebrate animal models [13]. Contributions from Eric Kandel and colleagues, showed that a simple behavioural reflex of the marine *Aplysia californica*, upon light stimulation, can be accompanied by a variety of learning events and long-term memory [7] [13]. This research revealed that even an animal with reduced number of nerve cells have remarkable behavioural and learning capabilities [14].

The early behavioural experiments in invertebrates led to the study of the same mechanisms in more complex animals. Vertebrates, specifically rodents, rapidly became the forefront of the neuroscience research as new genetic tools were developed. Engineered viruses have been produced to manipulate neuronal populations [15], allowing the tracing and delivery of transgenic material to neurons [16]. These techniques facilitated the study of neurobiological processes in a variety of behavioural experiments.

Pavlovian or classical conditioning is a particularly helpful behavioural paradigm to explore the mechanisms of learning and memory [17]. It elicits a measurable behavioural response through the associative learning of two distinct events. In the case of fear conditioning (FC), learning of a stimulus is associated with a negative outcome [18]. This form of conditioning received particular attention since it is conserved in many mammals' defensive behaviours, essential for survival [19]. Thus, it is used as a powerful tool to identify the early processing and storage of fear memories.

In a FC experiment, the animal is exposed to a neutral conditional stimulus (CS) - either a specific context or an auditory tone - together with an aversive unconditional stimulus (US) - an electrical foot shock. The association between these two events results in the subsequent expression of a fearful reaction, even in the absence of the US [20]. To trigger this response, after the CS-US learning task, animals are placed back in the same context testing contextual FC or, alternatively, exposed to the tone in a different context to induce cued fear conditioning [21].

Extensive research supports the convergence and processing of the tone-conditioning in the amygdala [19] [22] [23]. Indeed, this brain region has an important role in the limbic system [24], which governs the emotional states in the brain. Particularly, the amygdala coordinates the automatic responses observed during freezing behaviour, a fearful response characterized by the absence of movement (Figure 1.2).

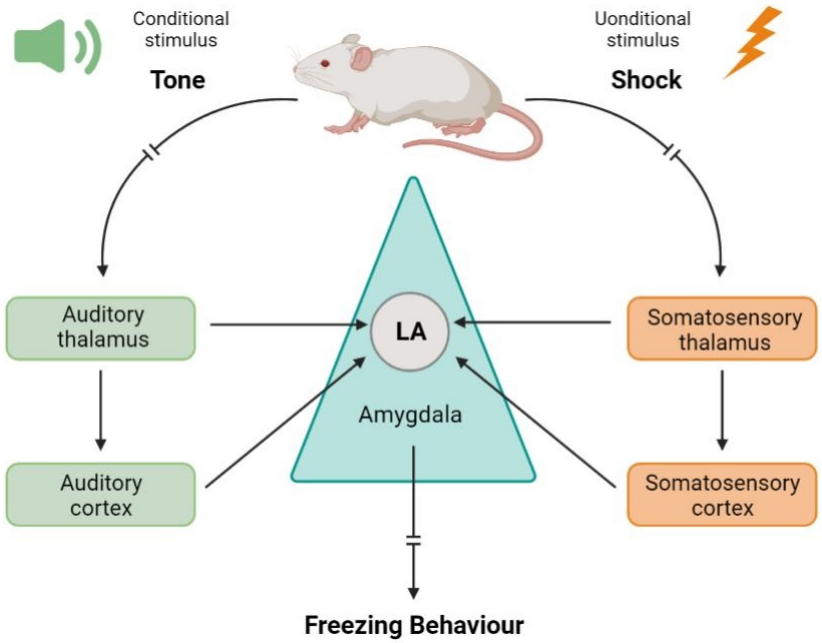

Figure 1.2: Neural circuits engaged in auditory fear conditioning. In an auditory fear conditioning protocol, both CS (tone) and US (shock) reach the LA from thalamic and cortical regions of the auditory and somatosensory systems, respectively. The CS-US convergence in the LA generates an automatic response from the amygdala whose projections reach brainstem areas (not shown) responsible for the expression of freezing behaviour.

During an auditory FC (aFC) protocol, sensory information related to the tone reaches the lateral nucleus of the amygdala from the auditory thalamus and cortex, via thalamic and cortical pathways [23]. Simultaneously, the amygdala integrates the painful experience related to the shock, with inputs from the somatosensory thalamus and cortex, resulting in the convergence of these two pathways [23]. Processing of information related to both events in the LA produces an automatic response upon re-exposure to the tone. The defensive response measured during freezing behaviour is conveyed by direct and indirect LA projections to the brainstem and hypothalamic regions [19].

Functional reorganization of brain networks during learning is essential to process the sensory information to recapitulate a memory. Early studies on the memory field show that no single memory centre exists in the brain. Instead, different brain regions of the nervous system participate in the representation of one single event [14]. Moreover, within each brain region, there is a constraint in the number of neurons that store information [25]. For example, despite being distinct types of memories, the proportion of LA neurons active during an aFC-induced fear memory is similar to the number of cells associated with a cocaine-cue memory [26] [27].

The subset of neurons, scattered in the brain, that are the substrate of a memory are known as the engram [28]. This term, first introduced by Richard Semon, refers to a functional population of neurons that encodes information in the brain, whose re-activation produces the recall of a memory [29]. As a result, it is essential to zoom at the level of the neuron to further understand what makes these cells eligible to store information (Figure 1.3).

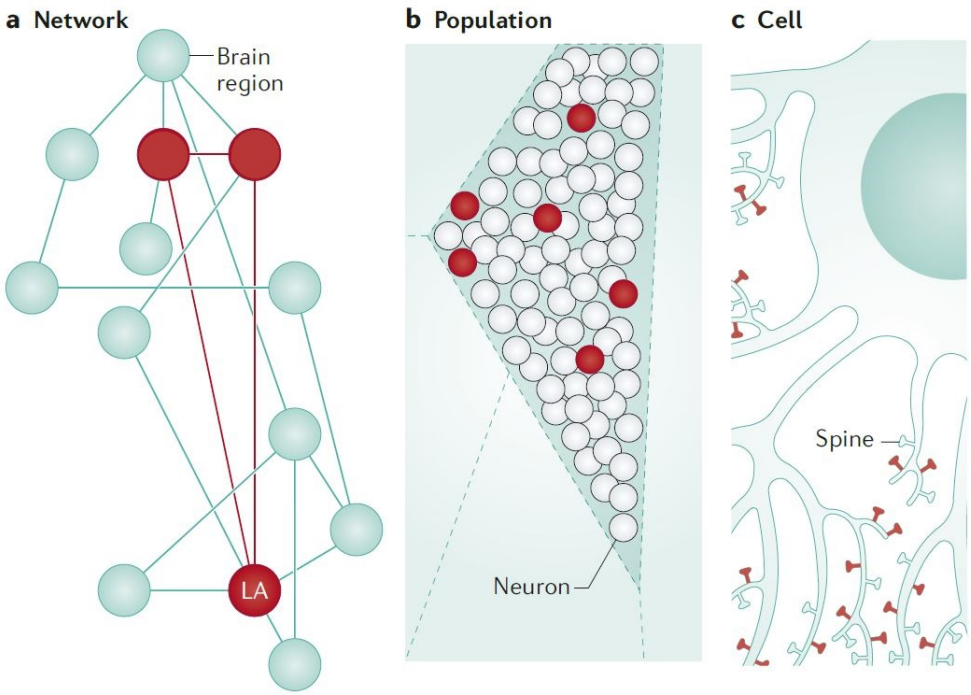

Figure 1.3: Levels of analysis of the memory trace. **a** Considering the engram of a fear memory as an example (shown in red), at the brain network level, several regions of the brain are engaged to represent the fear memory. Cyan lines illustrate the anatomical connections in the brain, whereas red lines depict the functional connection between the regions engaged to represent the fear engram. **b** Looking at the population of neurons within these brain regions, only a subset of cells is involved in engram representation. **c** Neurons that are part of the engram may display changes in their pattern of connectivity, for instance changes in dendritic spines. *Adapted from Josselyn et al, 2015* [16]

To identify the engram, Semon defined four criteria – persistence, ecphory, content, and dormancy [16] [29]. In more detail, an engram is a persistent physical change in the brain resulting from an experience. Engram cells have the potential for ecphory; in other words, the engram is expressed behaviourally by interacting with retrieval cues, such as sensory information related to the experience. Moreover, the content of the engram reflects the information that was processed during learning and predicts the subsequent retrieval of that information. Finally, an engram can be in a dormant state characterized by low neuronal activity, as opposed to the active state observed during memory expression.

Importantly, neuronal activity induces a cascade of intracellular signalling that leads to the expression of portions of the DNA sequence as a set of instructions for cellular function [30]. Immediate-early genes (IEGs) are transcribed encoding structural proteins, signaling molecules, and transcription factors (TFs) [31]. Particularly, *Fos* and *Arc* IEGs are rapidly induced in response to neuronal activation [32]. Its expression is used to visualize active neuronal populations in the brain of animals, and a powerful method to identify the neurons active during learning and memory [16] [33]. However, the expression of IEGs is transient since mRNA located in the nucleus, and protein levels in the cytoplasm, return to baseline within minutes and hours, respectively [34]. Thus, detection must be assessed respecting its window of compartmentalized expression. This molecular feature allows the selective tagging and study of the neuronal ensemble during different phases of the memory process.

1.2 Memory formation: from short to long-term memories

With the tools to find the engram, memory formation can be traced at different stages: encoding, consolidation, and retrieval. The encoding phase encompasses the early processing of information related to an experience or event, when memory remains in a fragile state - recent memory [16]. Through the process of consolidation, the engram becomes more resistant to disruption until consolidated as a long-term memory - remote memory [14].

Multiple studies have been highlighting the differences between keeping information temporary in our minds, such as the name of a street, and remembering something long-term, for instance our email address. The clinical history of the patient H. M. opened new avenues for the study of memory consolidation and the brain structures involved in this process [14]. Patient H. M. suffered from profound recent memory disability without apparent intellectual and long-term memory impairment, supporting the existence of distinct memory processes.

At the molecular level, behavioural studies using protein synthesis inhibitors, first indicated that newly synthesized proteins are required for long-term, but not short-term, memory storage [35]. On the basis of short-term memory, modification of pre-existing structural proteins and strengthening of pre-existing synaptic connections is required to retain information [36]. It is also through a recycling mechanism that IEGs are rapidly induced upon neuronal activation. IEGs rely on transcription factors constitutively expressed such as CRE-binding protein (CREB) (Figure 1.4 a). CREB binding to the cAMP response element (CRE) sequence in the DNA, rapidly drives the transcription of IEGs [31].

On the other hand, structural plasticity that accompanies long-term memory storage requires new protein synthesis as a result of *de novo* gene expression [37]. Although the molecular cascade is not fully characterized, neuronal activity induces cAMP production triggering protein kinase A (PKA) expression. This protein is transported from the synapse to the nucleus of the neuron, resulting in the phosphorylation of CREB [38]. CREB serves as a substrate for the transcription of a second messenger of transcription factors. The latter are responsible for inducing a new wave of gene expression [39], whose effector molecules are essential for strengthening the synaptic connections between neurons (Figure 1.4 b).

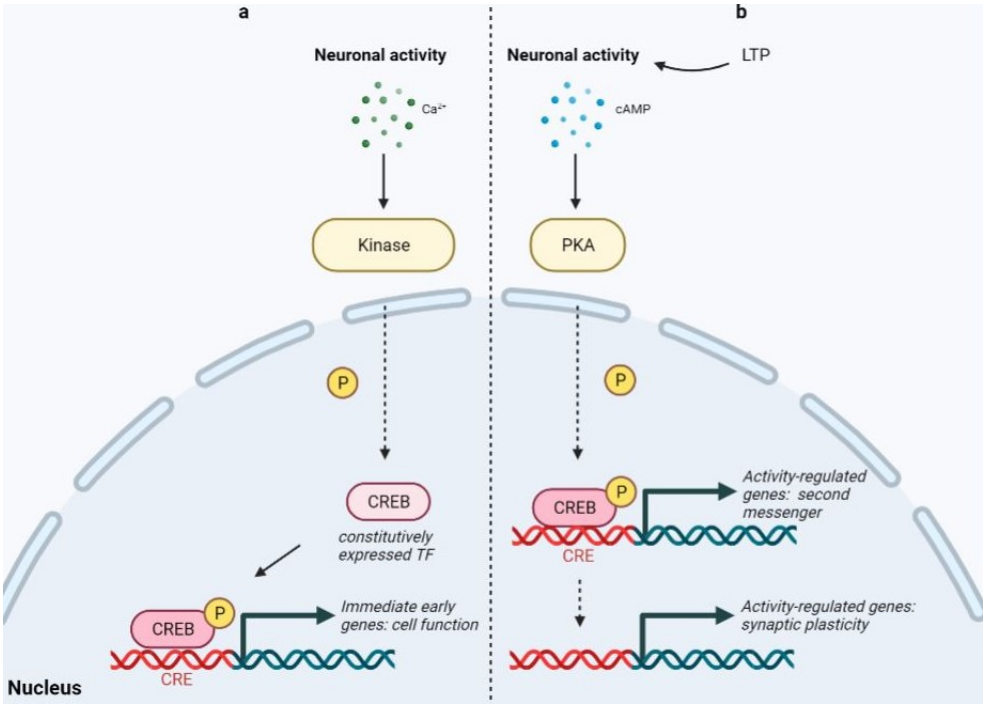

Figure 1.4: CREB-mediated gene expression. **a** Upon neuronal activity (Ca^{2+} influx), constitutively expressed transcription factor CREB, is rapidly phosphorylated (P) by kinases such as MAPK and CaMKII. CREB binding to the CRE in the DNA sequence induces the expression of immediate-early genes with specific cellular functions. **b** LTP induces messenger cAMP to activate PKA, which is transported from the synapse to the nucleus of the postsynaptic neuron, activating CREB. CREB induces the expression of effector molecules and inducible TFs which initiate a second wave of gene expression that supports synaptic plasticity.

1.3 Neuronal selection: the process of memory allocation

Advances were made to uncover the mechanisms underlying the different phases of memory formation. However, less is known about the selection of neurons to engage in this process. Interestingly, in the rodent LA, around 70% of neurons receive the sensory input related to both CS and US. Nevertheless, only one-quarter of these cells supports engram formation [40]. It seems that, despite a large number of neurons is responsive to stimuli, only a subset undergoes the molecular changes necessary for memory function [24]. This evidence suggests that only a portion of neurons is eligible to encode a memory.

To explain neuronal selection, studies have highlighted the role of higher CREB function and neuronal excitability at the time of encoding. These features were shown to increase the probability of neurons to represent the memory trace [27] [41] [42]. Particularly, in a paper by Han J. *et al.*, the authors used the expression of *Arc* as a fear memory marker. After injecting a viral vector encoding CREB in a subset of LA neurons, infected cells were more likely to be recruited during tone-conditioning [27]. Notably, increase in CREB function enhanced neuronal selection at the time of learning, but not after consolidation. Moreover, decreasing CREB in a similar proportion of LA neurons shifted the detection of Arc^{+} nuclei to the non-infected population.

Interestingly, the number of neurons that compose the memory trace was conserved throughout the experiments, independently of CREB manipulations. This data points to a competition between neurons during allocation that governs its selection. Supporting this hypothesis, lateral inhibition was proposed

as a model to constrain the engram size. During conditioning, it was shown that active neuronal populations inhibit non-active neurons in a process that limits the number of cells recruited, and stabilizes the memory [43] [44].

The findings that CREB is involved in neuronal allocation were consistent with experiments on the inactivation [41] or deletion [45] of CREB-infected neurons in the LA. By inactivating CREB$^+$ cells 30 minutes (min) before retrieval of a fear memory, researchers observed a decrease in its recall [41]. In a different study, neurons overexpressing CREB were silenced post-training, causing profound memory loss [45], whereas random ablation of a similar number of LA neurons did not disrupt memory function.

Electrophysiological studies also propose the recruitment of neurons based on the relative increase in excitability, immediately before learning [41] [42]. Importantly, CREB-infected neurons were shown to be more excitable that their neighbouring cells [41]. The enhanced intrinsic excitability of CREB$^+$ neurons conferred an advantage during the allocation of a fear memory. Also, increased excitability, without directly manipulating CREB function, was sufficient to bias neuronal allocation and enhance memory formation [42]. Studies in other brain structures and a variety of learning paradigms support the conservative nature of this mechanism [46] [47] [48].

The process that defines the allocation of information within a neural network is critical for the efficient storage and recall of that information [49]. At the time of encoding, neurons that display specific molecular and electrophysiological signatures are preferentially selected to be part of the engram. To acquire such features, neurons present specific genetic programs that define what it expresses at a specific time. As a result, mechanisms that regulate gene expression establish positive and negative transcriptional responses thereby influencing gene expression and defining neuronal function. One way to modulate the patterns of gene expression is through epigenetic mechanisms.

1.4 Epigenetics: the histone acetylation toolkit

The term “epigenetics” was first introduced by Conrad Waddington to define “the interactions of genes with their environment which brings phenotype into being” [50]. Currently it is commonly described as the alterations of gene expression that are independent of changes in the DNA sequence [51].

In eukaryotic cells, the genetic material is packed in the nucleus into a chromatin conformation. Chromatin can assume a more relaxed, transcriptionally active euchromatin, and more condensed, generally inactive heterochromatin. There are two main epigenetic mechanisms that influence gene expression: DNA methylation [52] and post-translational modifications (PTMs) of histones [53].

Histones are positively charged proteins responsible for packing DNA into a chromatin structure. Through electrostatic attraction or repulsion of histones to the negatively charged DNA backbone, a chromatin can adapt a more close or open conformation at specific sites of the DNA. There are two types of histones: linker histones (H1), and core histones (H2A, H2B, H3, and H4) [54]. The latter constitute octamers whose N-terminal tails ($\sim$ 40-50 amino acids) can be subjected to post-translational modifications [54]. Acetylation of lysine residues is one of the best characterised PTMs on histones tails [55], occurring in all core histones.

To regulate the acetylation levels, there are two groups of enzymes at play, HATs and HDACs [56]. Using acetyl coenzyme-A (acetyl-CoA) as the acetyl donor, HATs add an acetyl group to lysine residues of histones [57]. As a result, the electrostatic repulsion between histones and DNA increases, thereby enhancing chromatin accessibility. On the contrary, HDACs induce a more compact chromatin conformation by removal of acetyl groups from the histone tails [58] (Figure 1.5). According to the acetylation state, a cell can integrate new information by changes in the chromatin structure, therefore altering the accessibility of genes to the transcriptional machinery [59].

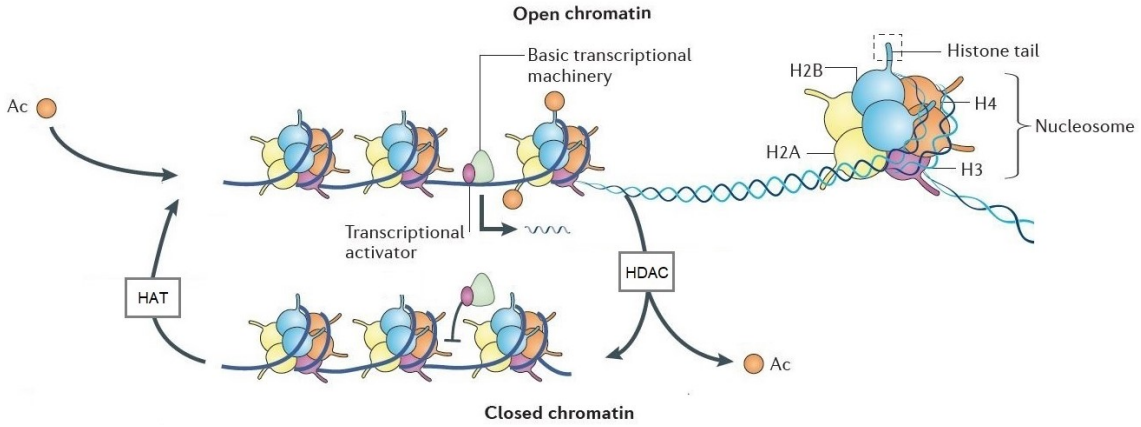

Figure 1.5: Regulation of histone acetylation. DNA is wrapped around an octamer of four core histones (H2A, H2B, H3, and H4) whose structure is organized by the linker H1 (not represented) in the nucleosome. Histone terminal tails project from the nucleosome and can be subjected to PTMs, namely acetylation. HATs add an acetyl (Ac) group to the histone tails opening the chromatin and allowing the basic transcriptional machinery to bind to activators in the DNA sequence. On the contrary, HDACs, by removal of an acetyl group, induce a more closed chromatin conformation at specific sites, decreasing the accessibility of the DNA to the transcriptional machinery. *Adapted from Gräff and Tsai, 2013* [55]

Increased levels of acetylation, in particular, are linked to transcriptionally active chromatin [60], providing binding surfaces for activators of gene expression [61]. Transcriptional activators in the DNA sequence, located close (promoters) or further (enhancers) to the transcription starting site of genes, are activated by binding to multiple TFs. In turn, transcription factors are induced by coactivators that often lack the specificity to bind to the DNA sequence, and together recruit RNA polymerase II to initiate gene transcription. The discovery that several coactivator proteins contain HATs activity, while repressors possess HDACs functions, further linked histone acetylation to transcriptional activation and deacetylation to gene repression [62].

1.5 Neuroepigenetics: role of acetylation in cognitive function

Recent discoveries on the broad field of epigenetics have highlighted the role of acetylation in cognition. A study by Levenson J. *et al.*, showed for the first time that learning triggers changes in acetylation levels following behavioural experiments [63]. After contextual fear conditioning, researchers observed increased acetylation of the histone H3 in neurons from the hippocamppus [63], a brain structure crucial for memory formation. Moreover, latent inhibition, a different form of associative learning, led to alterations of the acetyl levels in the histone H4 but not H3 [63]. These observations suggest that distinct memories are associated with specific patterns of histone modifications.

To understand whether increased acetylation supports memory formation, disruption of HATs activity is expected to interfere with memory processes. Indeed, several studies focusing on CBP, a transcriptional coactivator of CREB from the p300/CBP family (Figure 1.6), confirmed this hypothesis [64] [65]. Oike and colleagues, generated a CBP-deficient mouse line to mimic the clinical features observed in Rubinstein-Taybi syndrome (RTS). RTS is a condition characterized by retarded development and mental function, caused by a mutation in the CBP gene [64]. Results show impairment in long-term memory, suggesting that CBP is necessary for normal memory function.

To go a step further and distinguish the role of CBP as a histone acetyl transferase critical for memory from its role in developmental processes, a more refined study was performed. For this purpose, experiments were conducted in mice carrying a CBP transgene that specifically blocked its HAT activity, resulting once more in impaired memory recall [65]. Interestingly, in the same study, normal phenotype was rescued by a HDAC inhibitor to restore the acetylation levels in the brain. Indeed, the role of HDACs, specifically HDAC2, has been shown to negatively impact memory formation and synaptic plasticity [66]. Together, the present data suggest that the behavioural effects upon HATs blocking were acute rather than an irreversible deteriorating of neuronal function. Further studies also provided evidence that CBP is involved in short-term memory [67], for instance, in LA-dependent fear conditioning [68].

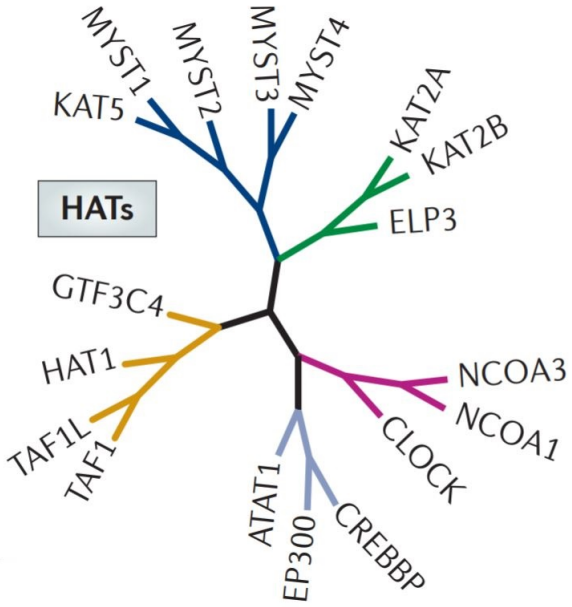

Figure 1.6: Phylogenetic representation of HATs enzymes. Different colored branches cluster proteins based on the similarity of their amino acid sequences. The phylogenetic representation clusters structurally (and sometimes functionally) related proteins. CREBBP (CBP) is part of the p300/CBP family (purple), whereas KAT5 is clustered in the MYST family (blue). *Adapted from Arrowsmith et al, 2012* [69].

From the MYST family (Figure 1.6), the activity of the histone acetyl transferase TIP60 (or KAT5) has also been thoroughly investigated [70]. In the brain, KAT5 has been linked to neuronal protection and survival [71], essential processes for neurons to engage in memory networks. However, the physiological function of KAT5 in the adult brain were challenged by the early embryonic lethality observed in TIP60-dificient mice. To gain insight into the role of KAT5 in memory formation, Uban *et al.* generated a conditional *Tip60* knockout mouse line [71]. Deletion of KAT5 in the hippocampus, in a controlled man-

ner, led to downregulation of genes necessary for synaptic plasticity, resulting in impairment of object recognition memory [71].

Regulation of the acetylation levels by HATs and HDACs has been highlighted by its different physiological functions, and because an imbalance of these groups of enzymes has been linked to multiple cognitive disorders. For example, several studies point to a decrease in the acetylation levels associated with the cognitive decline in Alzheimer's disease (AD) [72], the most common type of dementia. The main hallmarks of the disease include accumulation of extracellular amyloid plaques, neurofibillary tangles, and neuronal loss [73]. Amyloid plaques are formed by deposits of the amyloid β peptide produced by the enzymatic cleavage of the amyloid precursor protein (APP) [73].

Interestingly, in an AD fly model, the loss of HAT activity of TIP60 was linked to enhanced APP-mediate neuronal death [74]. Also, APP-overexpression in mouse neuronal cultures resulted in lower H3 and H4 acetylation, and decreased CBP levels [75]. Conversely, decrease of HDAC2 content in the hippocampus of CK-p25 AD mouse model, which recapitulate the major neuropathological characteristics of the disease, restored the acetylation levels and memory deficits [72]. The physiologic rescue was not associated with an increased number of neurons, supporting that the cognitive improvement does not require the production of new neurons to replace the neuronal loss.

Nonetheless, evidence on the acetylation levels associated with AD is ambiguous, since it was also reported an acetylated H3 increase in the *post mortem* brains of Alzheimer's patients [76]. Further investigation on the function of HATs and HADCs, specifically in the early stages of memory formation, is essential to detect epigenetic alterations associated with the cognitive impairments in AD in order to develop new therapeutic targets for these patients.

In summary, epigenetic regulation of gene expression is a dynamic process established by HATs, which create a permissive transcriptional state favouring neuronal function, and HDACs, whose imbalance negatively impacts memory. The role of acetylation in memory allocation determines the fate of a memory, thus it is an essential mechanism in memory processes that needs further investigation.

Aims

Long-lasting memories are represented by a sparse population of neurons, scattered in different brain regions, as a result of *de novo* gene expression. During the initial processing of information, only a subset of neurons is recruited to represent the engram. Evidences have pointed to a competitive advantage during memory allocation based on specific features that postsynaptic neurons display at the time of encoding. Furthermore, studies indicate a constant proportion of neurons, within each brain region, that represent the memory trace, supporting that engram allocation is not randomly solved.

Whether to acquire specific features to be eligible to be part of the engram or to express the genetic material necessary for long-term memory, the accessibility of specific genetic material is essential to drive the transcriptional responses for neuronal function. Taking this into consideration, we hypothesized whether the epigenome has a role in memory allocation by creating a more permissive structure for gene expression. Although the mechanisms of gene expression associated with memory formation are not fully characterized, the epigenetic code might elucidate how neurons integrate new information at the molecular level that result in changes in cellular function, while simultaneously being dynamic throughout time.

To test the hypothesis that epigenetic signatures confer an advantage during neuronal allocation, the present work will focus on histone acetylation. This PTM is one of the main epigenetic mechanisms studied in learning and memory. For this, acetylation levels will be increased by lentivirus (LV)-mediated overexpression of CBP and KAT5 in a subset of excitatory lateral amygdala neurons. Using KAT5, a more general acetyl mark, in addition to CBP known to be specifically recruited by CREB, uncovers the specificity of HATs that play a role in this process.

To investigate the influence of HATs in the recruitment of neurons to represent a fear engram, an auditory fear conditioning will be performed. Colocalization studies will be used to determine whether HATs-infected neurons are more represented in the memory trace, while keeping the engram size. Does our manipulation increase the baseline acetylation levels of HATs-infected neurons? To answer this question, histone 3 lysine 27 acetylation (H3K27ac) will be quantified as a proxy of the acetylation levels in the nuclei of both infected and non-infected neurons in the LA. After examining the recruitment of these two population of neurons during learning, the behavioural outcome of increased acetylation will be analyzed by recall of the fear memory.

Finally, to strengthen the hypothesis and understand if neurons can respond differently according to their epigenetic state, a hypoacetylated state will be induced in the same brain region by HDAC2-overexpression. With this experimental approach, we aim to comprehend the contribution of pre-learning increased acetylation in memory allocation, thus providing an insight on the upstream regulators of memory formation.

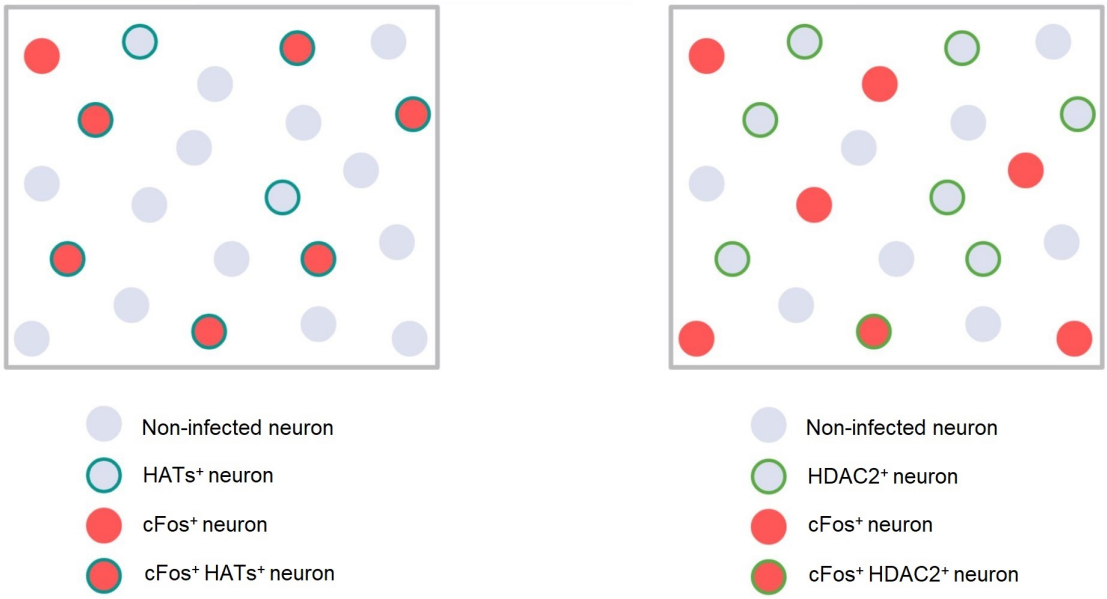

Figure 2.1: Hypothesis of memory allocation according to the acetylation levels of LA neurons. Increased aceylation in a subset of neurons by HATs-overexpression confers an advantage during the allocation of a fear engram (cFos$^+$ neurons). Thus, the proportion of double positive neurons (cFos$^+$ HATs$^+$ neurons) within the engram population is higher than in control (left). Conversely, decreased acetylation in HDAC2-infected neurons directs engram allocation to the non-infected population, manifested by a low colocalization of cFos$^+$ HDAC2$^+$ neurons that are part of the engram (right).

Materials and Methods

3.1 Animals

All experiments were performed on 8-week-old C57BL/6Rj male mice obtained from Janvier Labs (Janvier Labs, France). Animals were delivered at 7 weeks of age and were allowed an acclimatization period of 1 week before manipulation. All mice were housed in groups of three or four animals at 22-25 °C/ 55% humidity on a 12 hour (h) light-dark cycle (light at 7AM), with food and water *ad libitum*. All procedures and animal care were accepted by the Vaud Cantonal Veterinary Office under licence VD-3412, approved by the Federal Food Safety and Veterinary Office of the Federal Council of Switzerland.

3.2 Stereotaxic surgeries

For HATs-overexpression experiments, the following lentiviral vectors were bilaterally injected in the lateral amygdala: *pLVX-CaMKIIα::eGFP* (control vector), *pLVX-CaMKIIα::CBP-Myc* (CBP vector), or *pLVX-CaMKIIα::KAT5-Myc* (KAT5 vector). For HDAC2 studies, two viral vectors were used: *pLVX-CaMKIIα::eGFP* (control vector) or *pLVX-CaMKIIα::HDAC2-Myc* (HDAC2 vector), injected into the same LA coordinates. Titration of the virus was previously tested, and viral stock solutions were diluted in buffer solution (0.5% BSA in PBS 1X) according to the viral concentration, to achieve 450 ng 0.5 μL^{-1} per injection site. The pLVX-puro lentiviral vectors were produced in-house by transfecting HEK cells with the corresponding plasmid. Genes of interest *Cbp* (Gene ID:12914), *Kat5* (Gene ID: 81601), and *Hdac2* (Gene ID: 15182) were cloned and expressed from a *CaMKIIα* promoter. To visualize transgenic expression *Myc-flag* or *eGFP* was fused to the 5' end of the DNA sequence.

3.2.1 Surgical procedure

In all surgical procedures, mice were deeply anesthetized by an intraperitoneal injection of a mix containing fentanyl (0.05 mg kg^{-1}, Sintetica), midazolam (5 mg kg^{-1}, Actavis), and medetomidin (0.5 mg kg^{-1}, Orion Pharma). Additionally, a solution of lidocaine (6 mg kg^{-1}, Streuli Pharma), and bupivacaine (2.5 mg kg^{-1}, Sintetica) was injected at the site of incision. Surgical tools were kept in aseptic conditions, mice hair was clipped around the surgery site, and eyes were hydrated using viscotears (Carbomerum 980 2 mg g^{-1}, Bausch+Lomb). At the end of the surgery, a reversal anaesthesia containing antisedan (2.5 mg kg^{-1}, Orion Pharma) was injected intraperitoneally, and animals were placed on a heating pad until being awake. Paracetamol (Dafalgan, UPSA) was administered (500 g 250 mL^{-1} per cage) in drinking water for $\sim$6 days.

3.2.2 Viral injection

Animals were positioned in the stereotaxic apparatus (Stereotaxic for Mouse, RWD Life Science). To ensure the skull was levelled, the height of bregma in relation to lambda was compared (difference

in mean $<$0.05 mm), and lateral distance from bregma ($\pm$1.3 mm) was also confirmed (difference in mean $<$0.05 mm). Bregma coordinates were used as a guidance for the LA coordinates (AP: -1.14 mm; ML: $\pm$ 3.45 mm; DV: -4.46 mm). Injections were performed using a glass pipette (intraMARK, 10 µL, BLAUBRAND) connected to a syringe and a stereotaxic micromanipulator (Kopf Instruments). To allow the tissue to accommodate, the tip of the needle was positioned 0.05 mm below the target coordinates during 1 minute (min) before the injection. A volume of 400 nL to 500 nL of the viral solution was bilaterally injected into the LA (100 nL min^{-1} per site). To minimize backflow and allow diffusion of the virus, after the injection was complete, capillary was kept in the site of injection for an additional 10 min before a slow withdrawal.

3.3 Auditory fear conditioning

Mice underwent a cued auditory fear conditioning (MultiConditioning System, TSE systems) 10 days after the lentiviral injections. Behavioural testings were carried out between 8AM and 12AM. In all experiments, conditioning and recall sessions occurred in two different contexts – context A and context B, respectively. Context A consisted of a squared chamber with grid floor and smooth walls, whereas context B was composed of a round box with striped walls, smooth floor, and vanilla scent. The protocol comprised a 2 min habituation to the context A followed by one exposure to the auditory tone (CS: 2800 Hz, 85 dB, 30 seconds (sec)) paired with a shock (0.2 mA, 2 last sec of the auditory tone), and a 30 sec pause before the end of the session.

One day after the conditioning session, mice were placed in a novel context B for 2 min to allow free exploration, and were re-exposed to the auditory cue without shock (CS: 2800 Hz, 85 dB, 60 sec) to measure freezing behaviour. Animals returned to their home cage after the behavioural sessions. Freezing was automatically calculated with an infrared beam detection system within the apparatus, and was quantified when absence of movement was detected for more that 1 sec.

3.4 Sample preparation

For histological analysis of the brain, 60 min following the conditioning session (aFC group) or recall session (recall group), mice were deeply anaesthetised by an intraperitoneal pentobarbital injection (150 mg kg^{-1}, Streuli Pharma), and perfused transcardically (4% paraformaldehyde (PFA), 1X PBS, pH= 7.4). Brains were removed, post-fixed (4% PFA, overnight at 4 °C), cryoprotected (30% sucrose, 1X PBS, 48 h at 4 °C), and kept at -80 °C. Brain sections of 25 µm were cut using a sliding cryostat (Leica Microsystems) focusing on the lateral amygdala from Bregma –0.23 and –2.79, according to the Allen Brain Reference Atlas [77].

3.5 Immunohistochemistry

Free-floating sections of the brains were incubated in blocking solution (1% BSA, 1X PBS, 0.3% Triton X-100, Sigma-Aldrich) for 1 h at room temperature, followed by incubation of the primary antibody in blocking buffer (1% BSA, 1X PBS, 0.1% Triton X-100) for 2 nights at 4 °C, under constant shacking. Sections were washed extensively (1X PBS, 0.1% Triton X-100), and incubated with the secondary antibody in blocking buffer (1% BSA, 1X PBS, 0.1% Triton X-100) for 2 h at room temperature. Following washes with phosphate buffer, brain sections were incubated with Hoechst 33342 (Life Technologies, 1:2500 dilution) in 1X PBS for 5 min at room temperature. Lastly, slices were washed with 1X PBS before mounting on Superfrost glass slides (Thermo Fisher Scientific) with Fluoromount mounting medium (SouthernBiotech). All antibodies used in immunofluorescence experiments can be found in Table 3.1.

Table 3.1: Antibodies used in immunohistochemistry experiments

Antibody	**Dilution**	**Source**
Goat anti-cFos	1:1000	Santa Cruz Biotechnology, Cat #52 AF488
Mouse anti-H3K27ac	1:1000	Active Motif, Cat #39685
Rabbit anti-Myc flag	1:1000	Abcam, Cat #ab9106
Donkey anti-goat Alexa Fluor 647	1:800	Thermo Fisher Scientific, Cat #A-21447
Donkey anti-rabbit Alexa Fluor 488	1:800	Thermo Fisher Scientific, Cat #A-21206
Donkey anti-rabbit Alexa Fluor 568	1:800	Thermo Fisher Scientific, Cat #A-10042
Donkey anti-mouse Alexa Fluor 647	1:800	Thermo Fisher Scientific, Cat #A-21571

3.6 Image analysis

For colocalization studies, images were acquired on a virtual slide microscope (VS120, Olympus) with a 20x objective. Quantification of H3K27ac expression was processed using confocal imaging (Upright Leica DM6 CS) with a 40x objective. Quantitative analysis of Hoechst, cFos, Myc, and H3K27ac-positive cells was conducted using QuPath v.0.2.1.

3.6.1 Quantification of cFos$^+$ LV$^+$ in LA neurons

The lateral amygdala region of the brain was manually annotated based on the Hoechst 33342 signal, following the Allen Brain Reference Atlas. Within the outlined structure, Hoechst-positive cells were automatically detected using a custom-built script for QuPath to optimize nuclei detection conserving the nuclei exclusion criteria. For colocalization analysis of cFos and LV-positive cells, a custom-built script based on threshold intensities was used. Threshold for each image were optimized to be higher than the mean nucleus intensity of 5 negative cells (background detections), and slightly lower than the intensity values of 5 low-positive detections (positive detections), for each channel. Detections were average over 3-8 sections per animal.

The percentage of viral infection and neuronal activation were calculated (Equation 3.1 and 3.2, respectively). The injected brain area was carefully screened for possible off-site infection and were excluded from the analysis upon misinjection of the LA. Colocalization of double positive neurons (cFos$^+$ LV$^+$) were normalized to cFos to determine the percentage of allocation of infected neurons within the engram population (Equation 3.3). Moreover, chance level was reported as shown in Equation 3.4. Chance ratio was assessed to determine the percentage of double positive neurons, independently of the injection and activation rates (Equation 3.5).

$$\%LV\ expression = \frac{LV^+}{Hoechst^+} \times 100 \tag{3.1}$$

$$\%cFos\ expression = \frac{cFos^+}{Hoechst^+} \times 100 \tag{3.2}$$

$$\%Alocation = \frac{cFos^+LV^+}{cFos^+} \times 100 \tag{3.3}$$

$$\%Chance\ level = \frac{cFos^+}{Hoechst^+} \times \frac{LV^+}{Hoechst^+} \times 100 \tag{3.4}$$

$$\%Chance\ ratio = \frac{cFos^+LV^+/Hoechst^+}{Chance\ level} \times 100 \tag{3.5}$$

3.6.2 Characterization of H3K27ac intensity

Imaging of H3K27ac expression was obtained using Leica confocal microscope. Z-stack images were taken with a 40x objective (format: 2048 x 2048; zoom factor: 3.5; speed: 600). Acquisition was performed in the middle z-position of the specimen to obtain a robust number of neurons, decreasing the variability across samples. Sequential scanning was acquired ”between frames” to avoid crosstalk of the fluorochromes recorded by the detection channels, as shown in Table 3.2.

Following cell detection as previously explained, cells were excluded according to Hoechst expression. A range of Hoechst intensity was defined to exclude high-intensity Hoechst signal, saturated cells that could represent glia or abnormal neuronal morphology. Low-intensity Hoechst-positive neurons were also filtered to exclude neurons that were in a different z-plane, therefore affecting the intensity signal of the other channels. Following the Hoechst-based filtering, double positive neurons (LV$^+$ H3K27ac $^+$) were analysed according to *Myc*/*eGFP* and H3K27ac expression.

Table 3.2: Settings for ”between frames” sequential scanning of confocal lasers.

Laser - sequence (seq) number	Secondary antibody (target)	Wavelength of detection
HyD1 - seq1	Hoechst (nucleus)	420-450
HyD1 - seq2	Alexa-488 (Myc/eGFP)	510-530
HyD3 - seq3	Alexa-647 (H3K27ac)	650-680

3.7 Statistical analysis

Statistical analysis were performed using Prism 9 software (GraphPad). Data is reported as ± standard error of mean (s.e.m.). Data distribution was not formally tested but was assumed to have a normal distribution. Only male animals were used in the experiments and were randomly assigned to the experimental groups. All statistical tests used are reported in the corresponding legends.

Results

4.1 Manipulation of LA neurons by HATs-overexpression maintains baseline behaviour

To explore the contribution of epigenetic mechanisms in memory allocation, we tested whether higher acetylation levels in neurons, at the time of encoding, confers an advantage during engram formation. For this, we increased the levels of HATs enzymes in a sparse population of LA neurons by expressing CBP and KAT5, both implicated in memory processes [64] [71]. Following the viral injections, leading to increased HATs expression in infected neurons, animals were submitted to an auditory fear conditioning. The LA is necessary for the processing and expression of fear memories, thus the effects of HATs-overexpression were later assessed on the fear engram.

Previous *in vitro* experiments were performed to confirm the transfectability of the viral constructs in hippocampal cultured neurons. Once the expression of the constructs was established in neurons (data not shown), we conducted *in vivo* experiments by bilaterally injecting the virus carrying the HATs of interest (LV-CBP or LV-KAT5) or a control virus (LV-eGFP) in the LA of wild-type mice (Figure 4.1 a). Because *CaMKII*α is recruited during encoding of fear memories [78], it was used as a promoter to drive the expression of the viral constructs in excitatory neurons. Additionally, *Myc-flag* was inserted in the constructs of CBP and KAT5 to visualize transgenic expression, whereas an *eGFP* reporter was added to the control vector (Figure 4.1 b).

Ten days after surgery, we performed a behavioural paradigm consisting of one exposure to an auditory tone paired with a mild shock (aFC group, Figure 4.1 c). The same stereotaxic surgeries were carried out in a group of mice not exposed to any behavioural experiments (home cage group, Figure 4.1 c), to account for the baseline neuronal activity.

Animals used in the following experiments did not express an abnormal phenotype after the stereotaxic surgeries. Furthermore, to exclude the possibility that prolonged HATs-overexpression would alter baseline behaviour, freezing was measured during the conditioning session. Notably, there were no significant changes in freezing time following HATs-injections compared to the eGFP-control (Figure 4.1 d). Moreover, during the behavioural session, LV-mediated CBP and KAT5 expression did not affect overall stress levels or locomotion, as pointed by the exploratory area and distance travelled, respectively (Figure 4.1 e).

These results indicate that overexpression of CBP and KAT5 does not alter physiological behaviour, and animals present a similar phenotype to the control mice during the conditioning session.

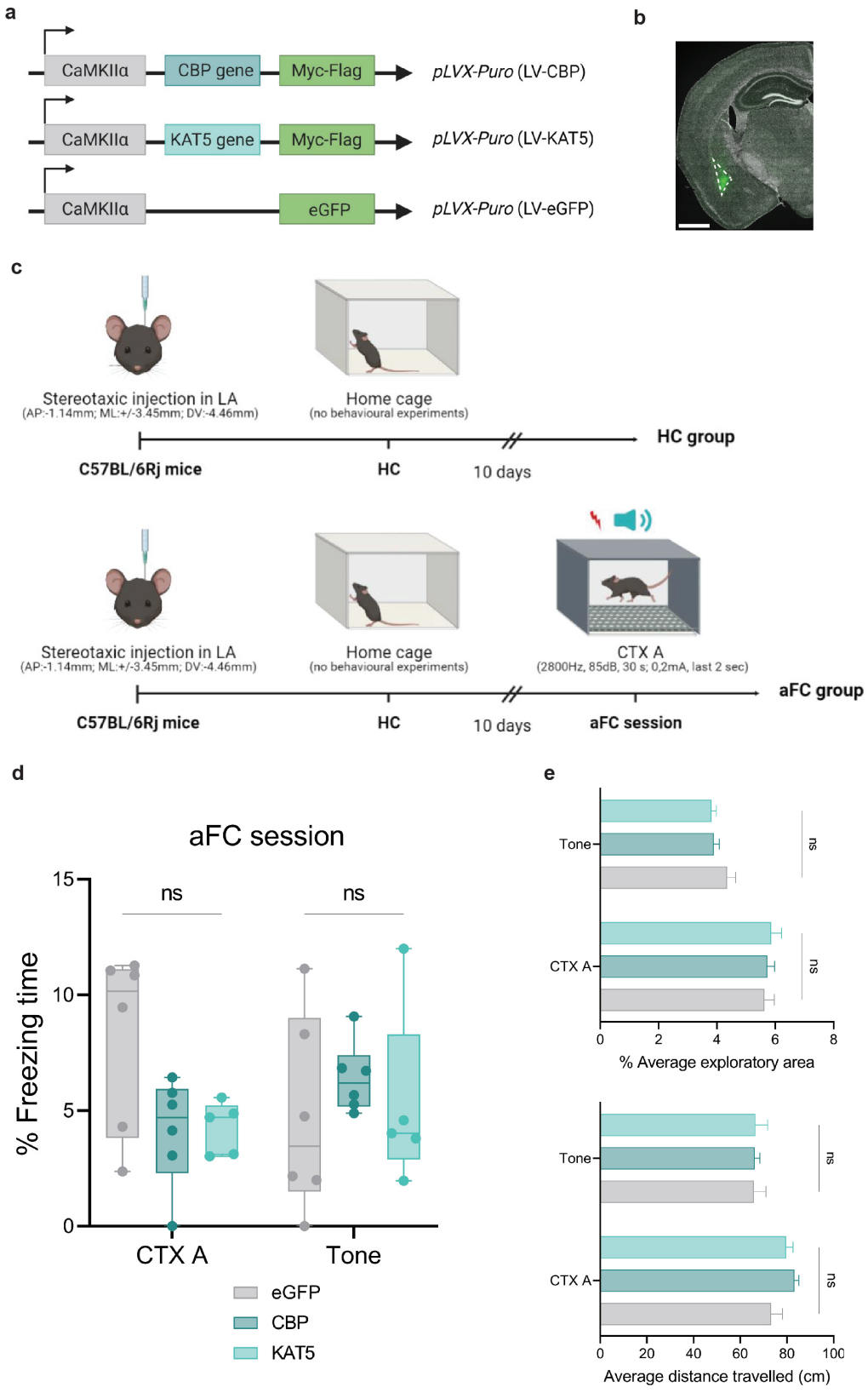

Figure 4.1: CBP and KAT5-injected mice in the lateral amygdala display a normal phenotype. a Scheme of the constructs used for the stereotaxic injections in the lateral amygdala. **b** Representative image of the viral expression in the LA. Scale bar 1 mm. **c** Schematic of the behavioural paradigm. Ten days after the stereotaxic injections, mice underwent an auditory fear conditioning (aFC group, *n= 17*). Control animals (HC group, *n*= 12) were not submitted to any behavioural experiments. **d** Average percentage of freezing response during the 2 min habituation to the context (CTX) A and the 30 sec presentation of the auditory cue (Tone), during the aFC session. Repeated measures (RM) two-way ANOVA, Šídák's multiple comparison test. **e** Average percentage of exploratory area (top) and average distance travelled (bottom), during CTX A and Tone presentation. RM two-way ANOVA, Tukey's multiple comparisons test. Data is represented as mean ± s.e.m. aFC, auditory fear conditioning; CTX, context; HC, home cage; LA, lateral amygdala; LV, lentivirus; ns, not significant.

4.2 *In vivo* CBP and KAT5-infected neurons are recruited to represent a fear memory

Once established that all animals expressed a similar phenotype during a learning task, we performed colocalization studies in the *post mortem* brains of the same animals. The analysis consisted on examining the population of neurons that composed the fear engram. Specifically, we assessed whether HATs-infected neurons were differently represented in the memory trace, compared to the eGFP-control.

Optimization of cell detection by a custom-built script from QuPath was essential to automatic and reliably identify the neurons that compose the lateral amygdala (Supplementary Figure S.1). Neurons active during the associative learning, constituting the fear engram, were visualized by the expression of cFos in the LA. Upon learning of the fear event, neuronal activity leads to a transient increase in cFos expression that can be detected by immunohistochemistry techniques [33].

Importantly, previous experiments in the lab identified that CBP and KAT5-transfected neuronal hippocampal cultures induce an increase in cFos expression 60 min following stimulation (data not shown). For this reason, 60 min after the behavioural session, animals were sacrificed to detect cFos expression during encoding of the fear memory (Figure 4.2 a). As expected, we observed a significant increase of $cFos^+$ cell density during tone-conditioning compared to home cage conditions in all groups (Supplementary Figure S.2). Importantly, independently of our manipulation, the overall size of the engram given by the proportion of active neurons in the LA, was not altered across the behavioural groups (Figure 4.2 b). These observations are consistent with previous studies, reporting that the number of neurons that represent the engram is restricted to a subset of cells, within each region of the brain [24].

If relative increase in acetylation bias LA neurons to participate in the fear engram, neurons overexpressing CBP and KAT5 are more likely to be active during the aFC session than eGFP-cells. Thus, to explore whether infected cells (LV^+) are preferentially engaged during learning ($cFos^+$), we determined the percentage of double positive neurons ($cFos^+$ LV^+) that compose the learning event. Interestingly, we discovered that CBP and KAT5-overexpressing neurons were more likely to be recruited to become part of the engram than $eGFP^+$ cells ($39.68 \pm 4.36\%$ and $50.32 \pm 2.64\%$ compared to $18.76 \pm 0.86\%$). It is important to highlight that the increased activation of HATs-neurons occurred during the encoding phase, but not in home cage conditions (Figure 4.2 c-d).

Despite the increased number of KAT5-infected neurons in the aFC group (Figure 4.2 e), the preferential allocation of the engram to $KAT5^+$ cells was not explained by the infection rate. With the chance ratio analysis, we detected an increased proportion of double positive neurons in HATs-injected mice submitted to the aFC (Figure 4.2 f), independently of the infection and activation rates.

Overall, these findings point to a competition between neurons to explain the allocation of a fear memory, a process that favours neurons with higher CBP and KAT5 content.

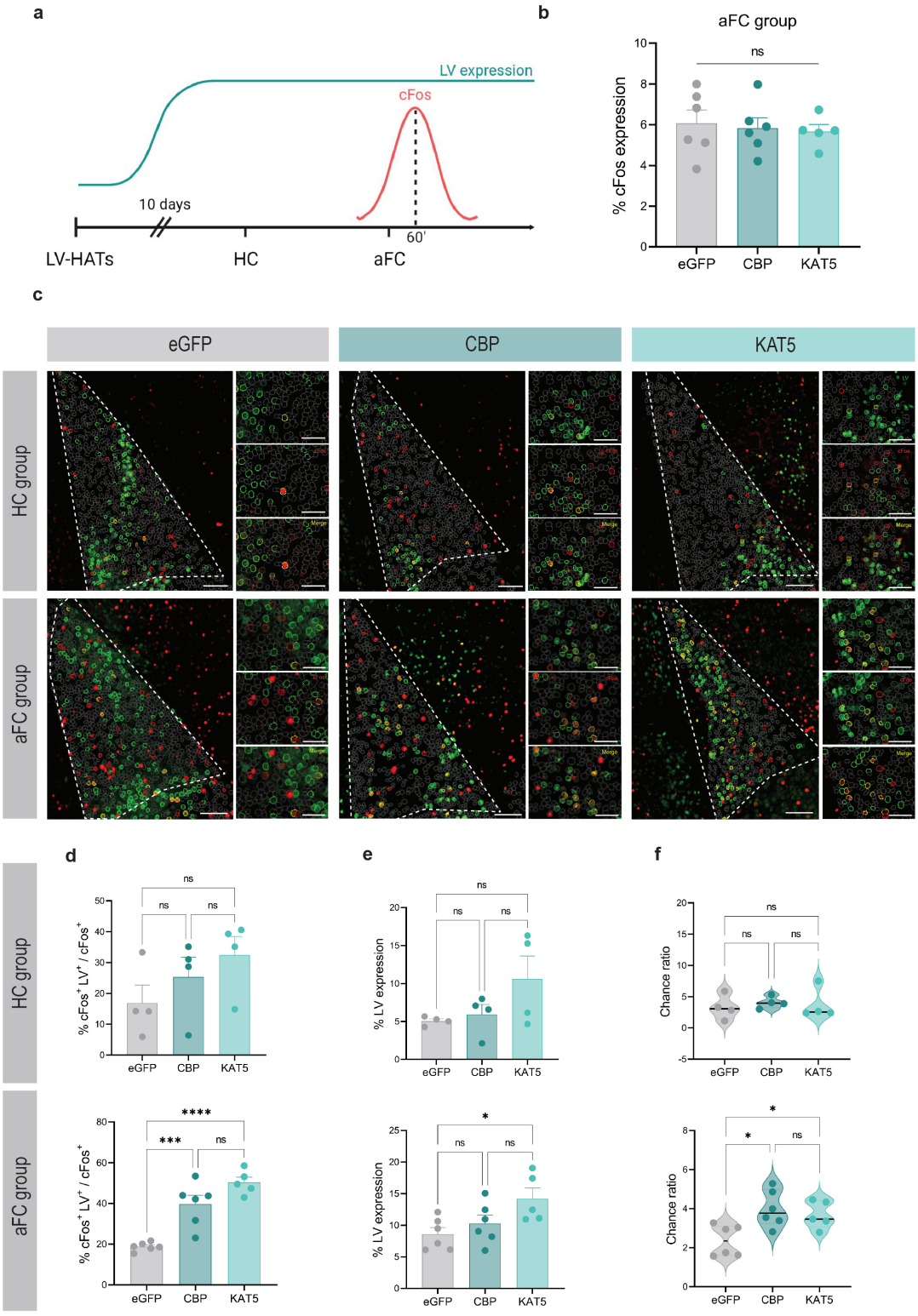

Figure 4.2: HATs-overexpression in the LA bias the recruitment of neurons into a fear memory. a Experimental schematic of the increased cFos expression in HATs-infected neurons, 60 min after the aFC session. **b** Quantification of active cells in the LA (cFos$^+$), 60 min after the conditioning session. Ordinary one-way ANOVA, Turkey's multiple comparisons test. **c** Representative fluorescent images of the colocalization of active (cFos$^+$) and infected (LV$^+$) neurons within the LA in the HC group (top) and aFC group (bottom). Cell detection surrounds the cells considered for the analysis. Green, infected neurons (LV$^+$); Red, active neurons (cFos$^+$); Yellow, merge (cFos$^+$ LV$^+$). Fluorescence microscopy, 20x. Scale bar: 100 µm (overview), 50 µm (close up). **d** Colocalization analysis of double positive neurons (cFos$^+$ LV$^+$) within the engram population in the HC group (top, *n*= 12) and aFC group (bottom, *n*= 17). Ordinary one-way ANOVA, ****P= 0.0001, ***P= 0.0005, Turkey's multiple comparisons test. **e** Quantification of infected cells (LV$^+$) in the LA region in the HC group (top) and aFC group (bottom). Ordinary one-way ANOVA, *P= 0.0285, Turkey's multiple comparisons test. **f** Chance ratio quantification in the HC group (top) and aFC group (bottom). HC: Ordinary one-way ANOVA, Turkey's multiple comparisons test. aFC: Ordinary one-way ANOVA, *P= 0.0129 (eGFP versus CBP), *P= 0.0386 (eGFP versus KAT5), Holm- Šídák's multiple comparison test. Data is represented as mean ± s.e.m. aFC, auditory fear conditioning; HATs, acetyl transferases; HC, home cage; LV, lentivirus; ns, not significant.

4.3 Nuclear expression of H3K27ac is higher in HATs-neurons

Previously we demonstrated that cFos expression is preferentially induced by CBP and KAT5-infected neurons. HATs can influence gene expression by activating transcription factors, such as CREB, functioning as coactivators of gene transcription [79]. Alternatively, HATs enzymes increase acetylation at the level of the histone tails altering chromatin conformation and thereby regulating the transcription of genes. To claim there is a preferential allocation of the fear engram within neurons with increased histone acetylation, it was essential to analyse the levels of acetylation at baseline.

In recent years, H3K27ac has been used as a reliable acetylation marker to distinguish transcriptionally active chromatin and active enhancers, from silent chromatin and inactive enhancers [80]. Also, increased H3K27ac expression in CBP^+ neurons was previously reported *in vitro* [81]. Considering the literature, to investigate whether epigenetic reprogramming plays a role in the relative increase of cFos expression in HATs-infected neurons, we determined the intensity of the histone marker H3K27ac as a proxy for the acetylation levels in both infected and non-infected neurons.

IHC experiments were carried out on brain sections from the HC group to detect the expression of H3K27ac in the lateral amygdala. To achieve higher resolution to quantify variations of H3K27ac expression in the nucleus, images were acquired using confocal microscopy (Figure 4.3 a). When plotting nuclei from mice according to the experimental groups, we found that HATs-positive cells expressed higher H3K27ac intensity compared to their neighbouring non-infected neurons (Figure 4.3 b). Conversely, H3K27ac expression was similar between $eGFP^+$ and $eGFP^-$ neurons in control mice. Interestingly, we noticed that the intensity range of H3K27ac was similar across all groups, however the distribution between the infected and non-infected population varied.

To confirm the robust increased intensity of H3K27ac between LV^+ and LV^- populations, data from the tested groups was analysed, individually. Once again, higher intensity of the acetylation marker was detected in CBP-infected neurons compared to the non-infected population (Figure 4.3 c). However, in the KAT5 group, H3K27ac did not accurately represented the infection rate previously calculated, since we detected a lower number of LV^- compared to LV^+ cells (Supplementary Figure S.3). For this reason, and due to the small number of replicates (Figure 4.3 c), further investigation regarding the acetylation levels in the KAT5 group should be assessed before drawing stronger conclusions.

Nonetheless, these results suggest an overall trend for the increased acetylation levels in HATs-cells compared to their neighbouring neurons, an epigenetic signature strongly present in CBP^+ neurons.

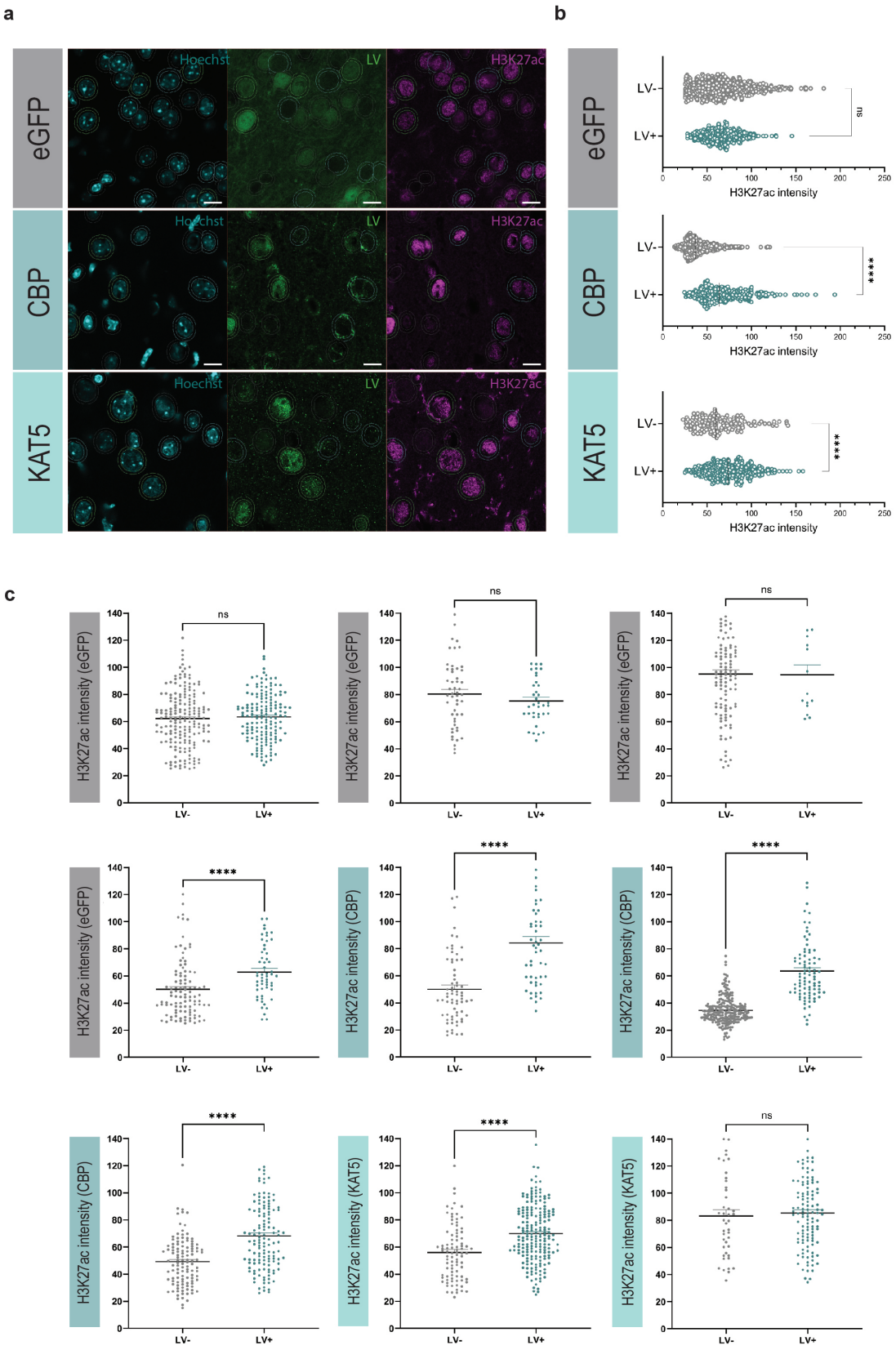

Figure 4.3: H3K27ac expression is increased in HAT-infected neurons. **a** Representative fluorescent images of Hoechst (nuclei), LV (infection) and H3K27ac (acetylation marker) in the HC group. Confocal 40x. Scale bar: 10 µm. **b** Group average of H3K27ac intensity in HC conditions. Each dot represents a neuron. Unpaired nonparametric, $^{****}P < 0.0001$, Mann-Whitney test. **c** Intensity of H3K27ac in neurons from each mouse, individually. Unpaired nonparametric, $^{****}P < 0.0001$, Mann-Whitney test. Data is represented as mean ± s.e.m. H3K27ac, histone 3 lysine 27 acetylation; HC, home cage; LV, lentivirus; ns, not significant.

4.4 CBP-injected mice freeze more during recent memory recall

Neurons overexpressing HATs, with higher acetylation levels, were more engaged during the encoding phase of memory formation. Next, we investigated if these modifications were sufficient to have a behavioural effect. Fearful memories are among the strongest and most persistent ways of learning [82]. Thus, we examined to which extend HATs-positive neurons, more recruited during learning, influenced recent memory recall.

To test this, we used the experimental setup of *in vivo* injections previously described. One day after the conditioning session in a context A, mice were placed in a novel context B to avoid contextual recall of the fear memory (Figure 4.4 a). Instead, animals were re-exposed to the tone responsible for the associative learning, resulting in the activation of the fear engram in the LA. Recall of the fear memory was assessed by measuring the percentage of time that animals spent freezing during tone presentation conducted 24h after conditioning.

Notably, CBP mice showed a significant increase in freezing compared to the control group (Figure 4.4 b), suggesting these animals successfully learnt the mild paradigm, and recalled the fear memory. In contrast, we found that the KAT5 group did not present changes in freezing time compared to eGFP animals. It is worth mentioning that no differences were detected in overall locomotion or stress levels as shown by the distance travelled and exploratory area, both similar across all groups during the recall session (Figure 4.4 c). Moreover, to ensure that all animals were able to participate in the fear learning, we observed the same parameters during the aFC session. Once again, animals exhibited a normal phenotype during the conditioning session (Supplementary Figure S.4).

A different behavioural paradigm could be performed to discriminate the freezing response to the novel context from the recall of the fear memory. Nonetheless, these results show an increase in memory performance in CBP-injected mice, but not in the KAT5 group, supported by the epigenetic reprogramming observed in CBP^{+} neurons.

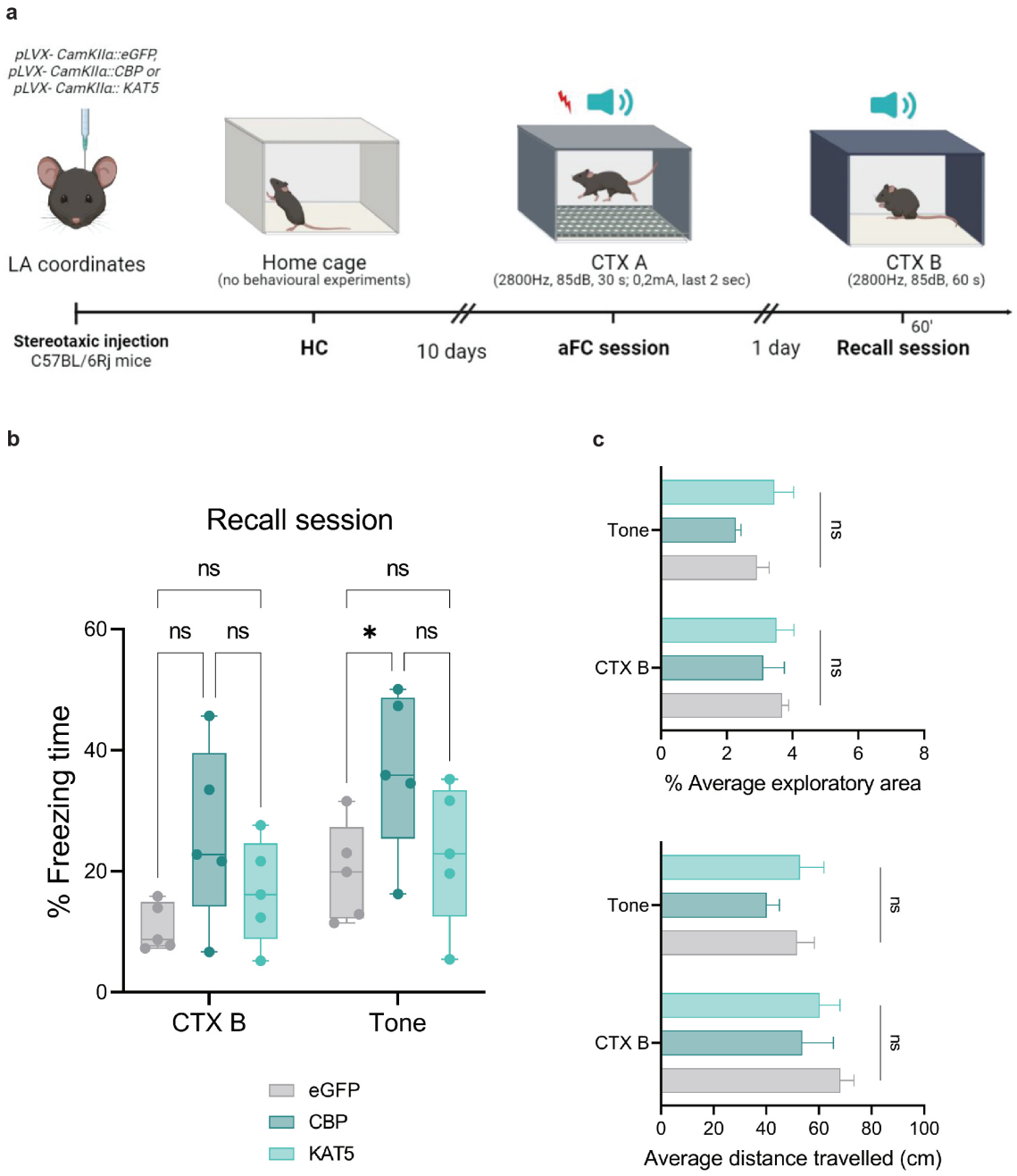

Figure 4.4: Fear memory recall is enhanced upon overexpression of CBP in the LA. a Experimental protocol for auditory fear conditioning designed to test cued fear memory. Animals injected with LV-CBP, LV-KAT5 or LV-eGFP into the LA, returned to their home cage after surgeries. Following the stereotaxic surgeries, animals underwent an auditory fear conditioning in context A (CTX A) consisting of one exposure to tone-shock. One day after the aFC session, animals were placed in a novel context B (CTX B) and fear memory was tested during tone presentation (recall group, *n*= 15). **b** Average percentage of freezing response during the 2 min habituation to the context B and the 60 sec of the auditory cue (Tone), during the recall session. RM two-way ANOVA, **P*= 0.0491, Šídák's multiple comparison test. **c** Average percentage of exploratory area (top) and average distance travelled (bottom), during CTX B and Tone presentation. RM two-way ANOVA, Tukey's multiple comparisons test. Data is represented as mean ± s.e.m. aFC, auditory fear conditioning; CTX, context; HC, home cage; LA, lateral amygdala; LV, lentivirus; ns, not significant.

4.5 Overexpression of HDAC2 in LA neurons alters the engram size

To further validate that increased acetylation levels in neurons modulate the allocation of a fear memory, we decided to challenge our hypothesis by overexpressing HDAC2 in LA neurons. With this manipulation, we aimed to induce a hypoacetylated state in the infected population, characterized by a more compact chromatin structure. Accordingly, we expected a shift to the non-infected neurons to represent the memory trace. Although HDAC inhibitors were shown to improve learning and memory storage, it is still lacking evidence whether there is a change in engram location, size and composition upon induction or silencing of HDAC enzymes.

For this, we injected *pLVX-CaMKIIα::eGFP* or *pLVX-CaMKIIα::HDAC2* in a subset of LA neurons (Figure 4.5 a), followed by a tone-conditioning session (aFC group, Figure 4.5 b). As previously described, animals were sacrificed 60 min after the behavioural session to detect learning-induced cFos expression. Additionally, we tested if early memory recall would be affected by HDAC2 overexpression, exposing animals to the auditory cue one day after the conditioning session (recall group, Figure 4.5 b).

In HC conditions, the number of active cells was identical between HDAC2 and eGFP-injected mice (Figure 4.5 c). Similar to what we previously observed, we found an increased number of cFos$^+$ neurons during the encoding phase compared to baseline conditions in the eGFP group (3.80 $\pm$ 0.69% compared to 7.45 $\pm$ 0.73%). Higher cFos expression accounts for the increased neuronal activity during the associative learning. Surprisingly, that was not the case in the HDAC2 group, showing a lower proportion of active cells than the eGFP group in the conditioning session (4.45$\pm$0.73% and 7.45$\pm$0.73%), as reported in Figure 4.5 c. Since the number of cFos$^+$ neurons was maintained, this data suggests that HDAC2-neurons did not participate in learning of the fear memory. Nevertheless, no behavioural differences were observed during the aFC session that could point to a disengagement during conditioning (Supplementary Figure S.5).

One limitation of the previous experiment is the different infection rates observed between eGFP and HDAC2 groups, displaying changes in the number of infected cells (Figure 4.5 d). Thus, for the allocation studies we determine the population of infected neurons that were activated during the aFC session, independently of the proportion of infected and activated cells. Although data shows an increase in double positive neurons between the testing groups in HC conditions, results indicate no differences in colocalization of cFos$^+$ LV$^+$ after the aFC session (Figure 4.5 e), in contrast to what reported upon HATs-overexpression.

To understand what are the implications of a reduced engram size behaviourally, we tested recent recall of the fear memory (Figure 4.5 f). Freezing behaviour in the eGFP group was comparable to what previously detected in HATs-experiments. Moreover, exposure to the tone did not alter freezing time in HDAC2-injected mice, as expected when retrieval of the fear memory takes place. Importantly, these results are not explained by changes in stress and locomotion, since no abnormal phenotype was present during the recall session in both testing groups (Figure 4.5 g).

Overall, and to our surprise, this data infers that HDAC2-overexpression destabilize the size of the engram by not participating in the fear learning in the first place.

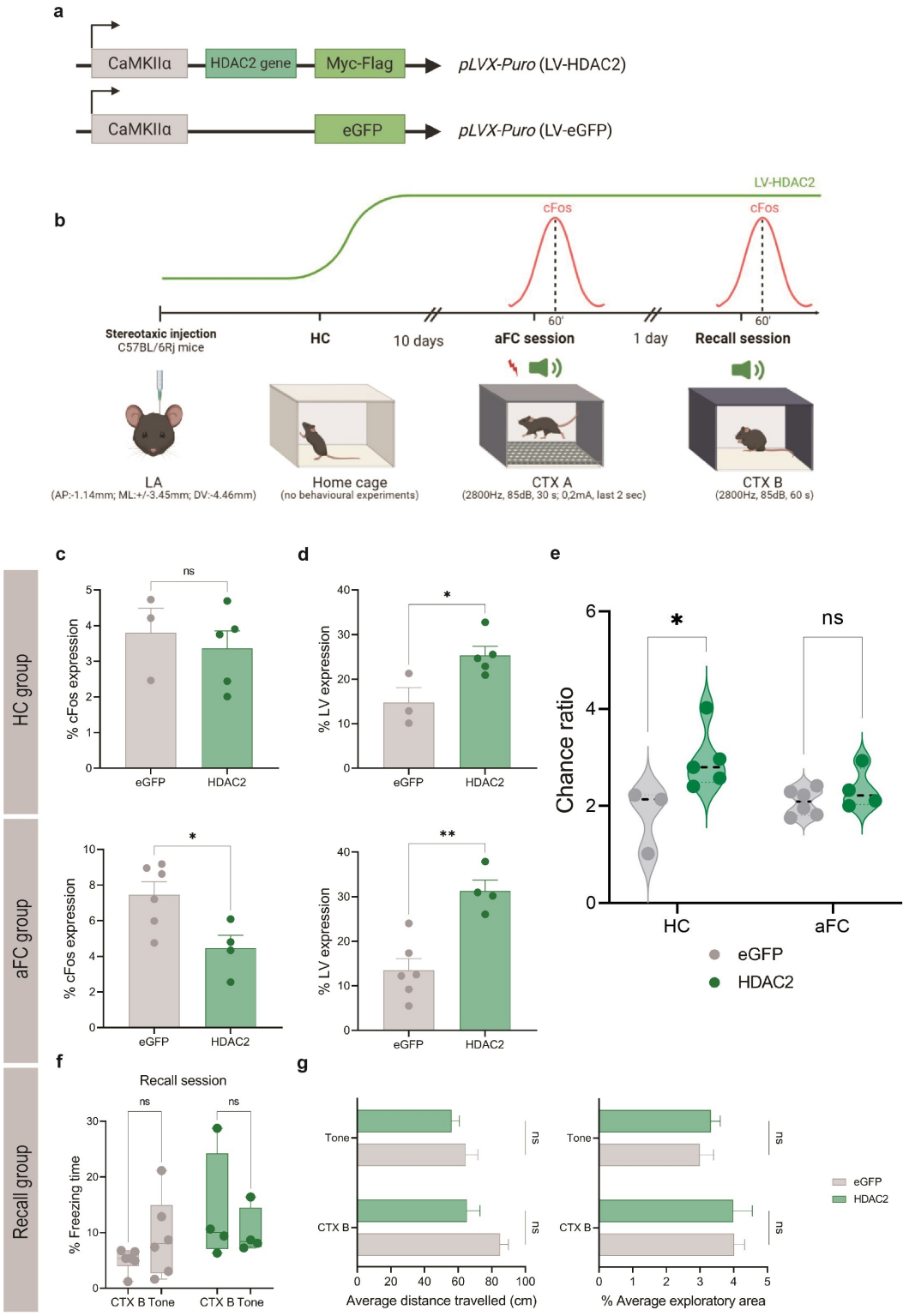

Figure 4.5: HDAC2-overexpression in LA neurons changes number of engram cells. **a** Schematic of the viral vectors encoding HDAC2 or eGFP that were injected in the lateral amygdala. **b** Protocol for the behavioural paradigm. Ten days after viral injections, mice underwent an aFC (aFC group, *n*= 10). An additional group was re-exposed to the tone one day after the conditioning session, in the absence of a foot shock (recall group, *n*= 10). Control animals did not undergo any behavioural experiments (HC group, *n*= 10). Animals were sacrificed 60 min after the behavioural session to detect cFos expression. **c** Percentage of activated cells (cFos$^+$) in the LA in the HC group (top) and aFC group (bottom). aFC: Unpaired t-test, **P*= 0.0243. **d** Proportion of infected neurons (LV$^+$) in the LA in the HC group (top) and aFC group (bottom). HC: Unpaired t-test **P*= 0.0268, aFC: Unpaired t-test, ***P*= 0.0017. RM two-way ANOVA, Šídák's multiple comparison test. **e** Chance ratio quantification of eGFP compared to HDAC2 animals in the HC and aFC groups. Ordinary two-way ANOVA, **P*= 0.0102, Šídák's multiple comparison test. **f** Average percentage of freezing response during the 2 min habituation to the context B and the 60 sec of the auditory cue (Tone), during the recall session. **g** Average distance travelled (left) and average percentage of exploratory area (right), during CTX B and Tone presentation. RM two-way ANOVA, **P*= 0.0491, Šídák's multiple comparison test. Data is represented as mean ± s.e.m. aFC, auditory fear conditioning; CTX, context; HC, home cage; LA, lateral amygdala; LV, lentivirus; HDAC2, histone deacetylase 2; ns, not significant.

Discussion

Morphological similar neurons display specific features that account for their preferential selection during memory allocation [27] [41] [42]. In the present study, we propose that during encoding, in order to constrain the engram size, there is a selection of neurons with higher histone acetylation as winners of the competition to allocate a fear memory.

Lentivirus have been reported to efficiently infected neurons with reduced inflammation [83], thus used as the viral vectors to drive the expression of CBP and KAT5 in a subset of LA neurons. To confirm the relative increased acetylation in HATs-infected cells, H3K27ac expression was quantified in LA neurons of home cage mice. In addition to be a robust acetylation marker, H3K27ac also identifies active enhancers and promoters [80], associated with increased gene expression. Our findings point to an increase in nuclear H3K27ac intensity by CBP and KAT5-overexpression, compared to their neighbouring cells. Importantly, to overcome the infected bias detected by H3K27ac in KAT5 animals, expression of a different acetyl mark is important to confirm higher acetylation levels in KAT5$^+$ cells. Acetylation marks identify changes in the epigenetic landscape and are dependent on the enzymes at play. KAT5, for example, was shown to target sites of H2 and H4 histones, which could be used to identify specific epigenetic signatures catalysed by this enzyme.

The effects of HATs-induced higher acetylation in memory allocation was assessed by submitting animals to an auditory fear conditioning. Detecting the expression of cFos during conditioning, identified the proportion of HATs$^+$ neurons that composed the fear engram. Remarkably, we show that HATs-infected cells were selected to constitute the engram population during learning of a fear memory. To our knowledge, this is the first description of a pre-learning acetylation contribution in the allocation process.

Consistent with previous studies, during HATs experiments the size of the engram was restricted to a similar number of cells, independently of the tested groups. If neuronal selection was a cell autonomous process, the number of cFos$^+$ neurons defining the memory trace would vary according to HATs manipulations. Since that was not the case, this data supports a competition between neurons that constrains the engram to a fixed population of active cells in the LA.

Interestingly, we noticed that the intensity range of H3K27ac marker was similar in all groups. These observations led us to speculate that there is an acetylation pool that can be randomly distributed between infected and non-infected neurons in eGFP mice or preferentially directed to the infected population upon HATs-overexpression. One possibility raised by these observations is that cellular metabolism may contribute to the predisposition of neurons to engage in memory formation. Because acetyl-CoA is the acetyl donor, a metabolic mechanism might also underlie the constraint in the acetylation levels in neurons. Indeed, it has been shown that hippocampal attenuation of an enzyme that generates acetyl-CoA for histone acetylation leads to defects in long-term spatial memory [84]. In our experiments, forcing the acetylation levels through CBP and KAT5 enzymes, imposes an epigenetic advantage in HATs$^+$ neurons to express cFos.

To further comprehend the mechanism of action of these enzymes, it would be important to assess genome-wide CBP and KAT5 histone acetylation patterns to discern the genes that are the targets of HATs enzymes. This would provide an insight into the expression of upregulated genes upon HATs induction. In particular, investigating whether acetylation marks are enriched at memory-related gene promoters and/or enhancers regions in the DNA sequence, would further support the correlation between increased acetylation and memory formation. Additionally, understanding if these genes are epigenetically altered early on in neurodegenerative diseases such as AD, would provide a clinical substrate for biomarkers of neurological diseases.

In line with the molecular changes observed upon HATs-overexpression, we consider its effects on memory recall. According to the ”priming” hypothesis, molecules that increase histone acetylation, enhance memory performance. First, there is an initial acetylation ”priming” of genes involved in memory. Upon neuronal stimulation, priming facilitates further acetylation thereby increasing gene transcription and enhancing memory during recall [85] [86]. Thus, we assessed the effects of a baseline increase in HATs enzymes in recent memory recall. Being a very mild event of one shock paired with a tone, we could discriminate if animals exhibit an enhanced memory retrieval.

Importantly, we verified that HATs manipulations did not alter overall behaviour during the associative learning. Behavioural analysis determined that all animals were exposed to tone-conditioning, similarly. During the recall session, upon re-exposure to the auditory cue, we observed a significant increase in freezing time in the CBP group, implying that animals recalled the fear memory. In contrast, the behavioural protocol did not alter freezing during the recall session in the KAT5 group compared to control. These findings indicate that the molecular changes observed on the engram composition were not sufficient to alter recent memory performance in KAT5-injected animals.

To further test the role of KAT5 in memory recall, a more complex protocol could be introduced. Exposing animals to tone-conditioning (CS+) and a different frequency-tone not associated with the shock (CS-), could be used to discern the specificity of the fear memory versus the generalization of fear upon exposure to the CS. Also, exploring the influence of higher acetylation during training in other types of memories, not restricted to fear conditioning, would provide evidence on the conservative nature of the acetylation process in neuronal selection.

As a proof of concept and to test the ability of neurons to respond differently according to their epigenetic state, we investigated the effects of lower acetylation in a subset of LA neurons. The acetylation profiling of neurons influences chromatin structure thereby altering gene expression. Although one would assume that HDACs have opposing effects to CBP and KAT5, this would be a broad assumption since not all members correlates with cognitive functions. Nonetheless, HDAC2 has been shown to reduce memory formation, whose effects are reversed upon treatment with HDAC inhibitors [66].

Considering the negative impact of HDAC2 in memory, we induced a hypoacetylation state in neurons by expressing this enzyme in the lateral amygdala, and investigated its effects on engram allocation and consequent behaviour. Surprisingly, after the behavioural session in HDAC2-injected mice, the size of the engram was similar to the one at baseline conditions, in contrast to what we observed so far. Our findings go against the initial hypothesis where we postulated that, upon HDAC2-overexpression,

the selection of neurons for engram representation would shift to the non-infected population. Instead, HDAC2 appears to destabilize memory by disrupting their allocation in the first place, pointing to a cell autonomous process that disrupts neuronal competition during encoding. Indeed, although not statistically significant, we propose there was a trend for decreased memory performance in HDAC2-injected animals during the recall session.

Although the number of infected neurons was significantly higher in HDAC2-injected animals than in control, no changes were detected in the recruitment of HDAC2^{+} cells into the fear memory, independently of activation and infection rates. These preliminary results open new avenues for investigating the mechanisms behind cognitive disorders that are influenced by a neuronal hypoacetylated state such as AD and RTS [56], and further support the importance of acetylation in memory functions.

Multiple studies suggest that during the early processing of information there is a bias of neurons with higher excitability immediately before training to be recruited for memory storage [41] [42] [48]. Thus, based on the intrinsic fluctuations of neuronal excitability, some neurons engage in storage of information. It is possible that the differences in HATs levels contribute to the diversity of firing properties in LA neurons. Thus, it seems imperative to conduct electrophysiological studies to test whether an increase in HATs function results in higher excitability of LA neurons, thereby mediating fear memory allocation. Indeed, preliminary experiments in the lab demonstrate that CBP and KAT5-infected neurons display a baseline increased intrinsic excitability that could support the eligibility of HATs cells to become part of the engram.

Together, these results point to a dynamic role of HATs and HDACs in establishing histone acetylation levels in neurons, and altering the engram and behaviour outcome, accordingly. Notably, we cannot exclude the possibility that other epigenetic mechanisms may also be predictive of the engram population. In fact, a recent study has proposed that the methylation state likely contributes to the excitability and recruitment of hippocampal cells to the neuronal ensemble [87]. Nevertheless, these results go in line with the hypothesis that HATs-infected neurons, with increased levels of histone acetylation than their identical non-infected cells, provide a substrate for memory allocation.

Conclusions

The competition to allocate the engram within a neuronal network is essential for the organization of a memory. In this study, we examined the epigenetic contribution of histone acetylation in the allocation of a fear engram. Histone acetylation has been shown to favour learning and memory, whereas the lack has been implicated in cognitive impairments. To our knowledge the influence of acetylation pre-learning and whether it confers an advantage during the early processes of memory formation was never formally tested.

Here, we show that expression of CBP and KAT5 in a subset of neurons induces a hyperacetylated state conferring an advantage during encoding. These manipulations did not affect the size of the engram, contrarily to HDAC2-overexpression, which destabilized the number of neurons activate during a learning event. Moreover, memory recall was positively impacted upon CBP-overexpression, supporting that increased acetylation pre-learning may prime neurons and enhance memory performance.

Although our findings provide compelling evidence that neurons with baseline higher HATs content are preferentially recruited into the memory trace, it remains unknown to what extent these findings recapitulated the physiologic mechanism of neuronal selection. Thus, future observational studies towards the discovery of the endogenous role of acetylation in memory formation, could open new avenues towards the discovery of epigenetic marks and upstream regulators of memory formation in both healthy and impaired brains.

Epigenetic mechanism continue to be revealed as important players of neuronal function, as well as implicated in a variety of neurological disorders. Either by constraining the engram size during encoding or by enhancing memory performance upon recall, acetylation changes in the brain influence a variety of cognitive functions. Understanding the rules of memory formation and establishing the role of acetylation in the allocation process, will provide insights into a range of neurological conditions characterized by a decline in one's ability to form new memories and/or recall old ones.

Bibliography

[1] M. Mesulam. From sensation to cognition. *Brain*, 121, (1998). doi: 10.1093/brain/121.6.1013.

[2] S. R. y Cajal. The Croonian lecture — la fine structure des centres nerveux. *Proceedings of the Royal Society of London*, 55, (1894). doi: 10.1098/rspl.1894.0063.

[3] E. G. Jones. Santiago Ramón y Cajal and the Croonian Lecture, March 1894. *Trends in Neurosciences*, 17, (1994). doi: 10.1016/0166-2236(94)90100-7.

[4] M. A. Nicolelis, E. E. Fanselow, and A. A. Ghazanfar. Hebb's dream: The resurgence of cell assemblies. *Neuron*, 19:219–221, (1997). doi: 10.1016/S0896-6273(00)80932-0.

[5] D. O. Hebb. *The Organization of Behavior; a neuropsychological theory*. Wiley, (1949).

[6] R. E. Brown. Donald Hebb and the Organization of Behavior: 17 years in the writing. *Molecular Brain*, 13, (2020). doi: 10.1186/s13041-020-00567-8.

[7] V. Castellucci, H. Pinsker, I. Kupfermann, and E. R. Kandel. Neuronal mechanisms of habituation and dishabituation of the gill-withdrawal reflex in *Aplysia*. *Science*, 167, (1970). doi: 10.1126/science.167.3926.1745.

[8] A. E. Pereda. Electrical synapses and their functional interactions with chemical synapses. *Nature Reviews Neuroscience*, 15, (2014). doi: 10.1038/nrn3708.

[9] B. Katz. *The release of neural transmitter substances*. Springfield, III., Thomas, (1969).

[10] T. Südhof. Neurotransmitter release: The last millisecond in the life of a synaptic vesicle. *Neuron*, 80, (2013). doi: 10.1016/j.neuron.2013.10.022.

[11] T. V. P. Bliss and T. Lømo. Long-lasting potentiation of synaptic transmission in the dentate area of the anaesthetized rabbit following stimulation of the perforant path. *The Journal of Physiology*, 232, (1973). doi: 10.1113/jphysiol.1973.sp010273.

[12] B. McNaughton and R. Morris. Hippocampal synaptic enhancement and information storage within a distributed memory system. *Trends in Neurosciences*, 10, (1987). doi: 10.1016/0166-2236(87)90011-7.

[13] E. R. Kandel. The molecular biology of memory storage: A dialogue between genes and synapses. *Science*, 294, (2001). doi: 10.1126/science.1067020.

[14] B. Milner, L. R. Squire, and E. R. Kandel. Cognitive neuroscience and the study of memory. *Neuron*, 20, (1998). doi: 10.1016/S0896-6273(00)80987-3.

[15] A. R. Nectow and E. J. Nestler. Viral tools for neuroscience. *Nature Reviews Neuroscience*, 21, (2020). doi: 10.1038/s41583-020-00382-z.

[16] S. A. Josselyn, S. Köhler, and P. W. Frankland. Finding the engram. *Nature Reviews Neuroscience*, 16, (2015). doi: 10.1038/nrn4000.

[17] I. P. Pavlov. Conditioned reflexes: An investigation of the physiological activity of the cerebral cortex. *Annals of neurosciences*, 17, (2010). doi: 10.5214/ans.0972-7531.1017309.

[18] R. C. Bolles and M. S. Fanselow. A perceptual-defensive-recuperative model of fear and pain. *Behavioral and Brain Sciences*, 3, (1980). doi: 10.1017/S0140525X0000491X.

[19] S. Maren. Neurobiology of pavlovian fear conditioning. *Annual Review of Neuroscience*, 24, (2001). doi: 10.1146/annurev.neuro.24.1.897.

[20] J. E. LeDoux. Emotion circuits in the brain. *Annual Review of Neuroscience*, 23, (2000). doi: 10.1146/annurev.neuro.23.1.155.

[21] R. G. Phillips and J. E. LeDoux. Differential contribution of amygdala and hippocampus to cued and contextual fear conditioning. *Behavioral Neuroscience*, 106, (1992). doi: 10.1037/0735-7044.106.2.274.

[22] J. E. LeDoux, C. R. Farb, and L. M. Romanski. Overlapping projections to the amygdala and striatum from auditory processing areas of the thalamus and cortex. *Neuroscience Letters*, 134, (1991). doi: 10.1016/0304-3940(91)90526-Y.

[23] L. M. Romanski, M.-C. Clugnet, F. Bordi, and J. E. LeDoux. Somatosensory and auditory convergence in the lateral nucleus of the amygdala. *Behavioral Neuroscience*, 107, (1993). doi: 10.1037/0735-7044.107.3.444.

[24] P. I. Yakovlev. Motility, behavior and the brain. *The Journal of Nervous and Mental Disease*, 107: 313–335, (1948). doi: 10.1097/00005053-194810740-00001.

[25] S. A. Josselyn and S. Tonegawa. Memory engrams: Recalling the past and imagining the future. *Science*, 367, (2020). doi: 10.1126/science.aaw4325.

[26] H.-L. Hsiang, J. R. Epp, M. C. van den Oever, C. Yan, A. J. Rashid, N. Insel, L. Ye, Y. Niibori, K. Deisseroth, P. W. Frankland, and S. A. Josselyn. Manipulating a ”cocaine engram” in mice. *Journal of Neuroscience*, 34:14115–14127, (2014). doi: 10.1523/JNEUROSCI.3327-14.2014.

[27] J.-H. Han, S. A. Kushner, A. P. Yiu, C. J. Cole, A. Matynia, R. A. Brown, R. L. Neve, J. F. Guzowski, A. J. Silva, and S. A. Josselyn. Neuronal competition and selection during memory formation. *Science*, 316, (2007). doi: 10.1126/science.1139438.

[28] R. W. Semon. *Mneme*. G. Allen Unwin ltd., The Macmillan company, (1921).

[29] D. L. Schacter. *Forgotten ideas, neglected pioneers: Richard Semon and the story of memory.* Psychology Press, (2001).

[30] W. Tischmeyer and R. Grimm. Activation of immediate early genes and memory formation. *Cellular and Molecular Life Sciences (CMLS)*, 55, (1999). doi: 10.1007/s000180050315.

[31] E.-L. Yap and M. E. Greenberg. Activity-regulated transcription: Bridging the gap between neural activity and behavior. *Neuron*, 100:330–348, (2018). doi: 10.1016/j.neuron.2018.10.013.

[32] M. Sheng and M. E. Greenberg. The regulation and function of c-fos and other immediate early genes in the nervous system. *Neuron*, 4:477–485, (1990). doi: 10.1016/0896-6273(90)90106-P.

[33] K. Minatohara, M. Akiyoshi, and H. Okuno. Role of immediate-early genes in synaptic plasticity and neuronal ensembles underlying the memory trace. *Frontiers in Molecular Neuroscience*, 8, (2016). doi: 10.3389/fnmol.2015.00078.

[34] J. F. Guzowski, B. L. McNaughton, C. A. Barnes, and P. F. Worley. Environment-specific expression of the immediate-early gene Arc in hippocampal neuronal ensembles. *Nature Neuroscience*, 2, (1999). doi: 10.1038/16046.

[35] H. P. Davis and L. R. Squire. Protein synthesis and memory: A review. *Psychological Bulletin*, 96: 518–559, (1984). doi: 10.1037/0033-2909.96.3.518.

[36] P. Goelet, V. F. Castellucci, S. Schacher, and E. R. Kandel. The long and the short of long–term memory — a molecular framework. *Nature*, 322:419–422, (1986). doi: 10.1038/322419a0.

[37] B. J. Bacskai, B. Hochner, M. Mahaut-Smith, S. R. Adams, B.-K. Kaang, E. R. Kandel, and R. Y. Tsien. Spatially resolved dynamics of cAMP and protein kinase A subunits in *Aplysia* sensory neurons. *Science*, 260, (1993). doi: 10.1126/science.7682336.

[38] P. K. Dash, B. Hochner, and E. R. Kandel. Injection of the cAMP-responsive element into the nucleus of *Aplysia* sensory neurons blocks long-term facilitation. *Nature*, 345:718–721, (1990). doi: 10.1038/345718a0.

[39] E. Benito and A. Barco. The neuronal activity-driven transcriptome. *Molecular Neurobiology*, 51: 1071–1088, (2015). doi: 10.1007/s12035-014-8772-z.

[40] S. Rumpel, J. LeDoux, A. Zador, and R. Malinow. Postsynaptic receptor trafficking underlying a form of associative learning. *Science*, 308, (2005). doi: 10.1126/science.1103944.

[41] Y. Zhou, J. Won, M. G. Karlsson, M. Zhou, T. Rogerson, J. Balaji, R. Neve, P. Poirazi, and A. J. Silva. CREB regulates excitability and the allocation of memory to subsets of neurons in the amygdala. *Nature Neuroscience*, 12, (2009). doi: 10.1038/nn.2405.

[42] A. P. Yiu, V. Mercaldo, C. Yan, B. Richards, A. J. Rashid, H.-L. L. Hsiang, J. Pressey, V. Mahadevan, M. M. Tran, S. A. Kushner, M. A. Woodin, P. W. Frankland, and S. A. Josselyn. Neurons are recruited to a memory trace based on relative neuronal excitability immediately before training. *Neuron*, 83, (2014). doi: 10.1016/j.neuron.2014.07.017.

[43] T. Stefanelli, C. Bertollini, C. Lüscher, D. Muller, and P. Mendez. Hippocampal somatostatin interneurons control the size of neuronal memory ensembles. *Neuron*, 89, (2016). doi: 10.1016/j.neuron.2016.01.024.

[44] D. J. Morrison, A. J. Rashid, A. P. Yiu, C. Yan, P. W. Frankland, and S. A. Josselyn. Parvalbumin interneurons constrain the size of the lateral amygdala engram. *Neurobiology of Learning and Memory*, 135, (2016). doi: 10.1016/j.nlm.2016.07.007.

[45] J.-H. Han, S. A. Kushner, A. P. Yiu, H.-L. L. Hsiang, T. Buch, A. Waisman, B. Bontempi, R. L. Neve, P. W. Frankland, and S. A. Josselyn. Selective erasure of a fear memory. *Science*, 323, (2009). doi: 10.1126/science.1164139.

[46] R. Czajkowski, B. Jayaprakash, B. Wiltgen, T. Rogerson, M. C. Guzman-Karlsson, A. L. Barth, J. T. Trachtenberg, and A. J. Silva. Encoding and storage of spatial information in the retrosplenial cortex. *Proceedings of the National Academy of Sciences*, 111, (2014). doi: 10.1073/pnas.1313222111.

[47] Y. Sano, J. Shobe, M. Zhou, S. Huang, T. Shuman, D. Cai, P. Golshani, M. Kamata, and A. Silva. CREB regulates memory allocation in the insular cortex. *Current Biology*, 24, (2014). doi: 10.1016/j.cub.2014.10.018.

[48] S. Park, E. E. Kramer, V. Mercaldo, A. J. Rashid, N. Insel, P. W. Frankland, and S. A. Josselyn. Neuronal allocation to a hippocampal engram. *Neuropsychopharmacology*, 41, (2016). doi: 10.1038/npp.2016.73.

[49] T. Rogerson, D. J. Cai, A. Frank, Y. Sano, J. Shobe, M. F. Lopez-Aranda, and A. J. Silva. Synaptic tagging during memory allocation. *Nature Reviews Neuroscience*, 15, (2014). doi: 10.1038/nrn3667.

[50] C. Waddington. The epigenotype. *International Journal Epidemiology*, 41:10–13, (1942).

[51] C. Wu and J. R. Morris. Genes, genetics, and epigenetics: A correspondence. *Science*, 293, (2001). doi: 10.1126/science.293.5532.1103.

[52] P. A. Jones and D. Takai. The role of DNA methylation in mammalian epigenetics. *Science*, 293, (2001). doi: 10.1126/science.1063852.

[53] A. J. Bannister and T. Kouzarides. Regulation of chromatin by histone modifications. *Cell Research*, 21, (2011). doi: 10.1038/cr.2011.22.

[54] R. D. Kornberg and Y. Lorch. Twenty-five years of the nucleosome, fundamental particle of the eukaryote chromosome. *Cell*, 98, (1999). doi: 10.1016/S0092-8674(00)81958-3.

[55] J. Gräff and L.-H. Tsai. Histone acetylation: molecular mnemonics on the chromatin. *Nature Reviews Neuroscience*, 14:97–111, (2013). doi: 10.1038/nrn3427.

[56] J. Gräff and L.-H. Tsai. The potential of HDAC inhibitors as cognitive enhancers. *Annual Review of Pharmacology and Toxicology*, 53, (2013). doi: 10.1146/annurev-pharmtox-011112-140216.

[57] C. E. Berndsen and J. M. Denu. Catalysis and substrate selection by histone/protein lysine acetyltransferases. *Current Opinion in Structural Biology*, 18, (2008). doi: 10.1016/j.sbi.2008.11.004.

[58] K. Ekwall. Genome-wide analysis of HDAC function. *Trends in Genetics*, 21, (2005). doi: 10.1016/j.tig.2005.08.009.

[59] S. K. Kurdistani, S. Tavazoie, and M. Grunstein. Mapping global histone acetylation patterns to gene expression. *Cell*, 117, (2004). doi: 10.1016/j.cell.2004.05.023.

[60] C.-R. C. Hebbes TR, Thorne AW. A direct link between core histone acetylation and transcriptionally active chromatin. *The EBMO Journal*, 7(5), (1988).

[61] M.-H. Kuo and C. D. Allis. Roles of histone acetyltransferases and deacetylases in gene regulation. *BioEssays*, 20, (1998). doi: 10.1002/(SICI)1521-1878(199808)20:8⟨615::AID-BIES4⟩3.0.CO;2-H.

[62] V. V. Ogryzko, R. Schiltz, V. Russanova, B. H. Howard, and Y. Nakatani. The transcriptional coactivators p300 and CBP are histone acetyltransferases. *Cell*, 87, (1996). doi: 10.1016/S0092-8674(00)82001-2.

[63] J. M. Levenson, K. J. O'Riordan, K. D. Brown, M. A. Trinh, D. L. Molfese, and J. D. Sweatt. Regulation of histone acetylation during memory formation in the hippocampus. *Journal of Biological Chemistry*, 279, (2004). doi: 10.1074/jbc.M402229200.

[64] Y. Oike. Truncated CBP protein leads to classical Rubinstein-Taybi syndrome phenotypes in mice: implications for a dominant-negative mechanism. *Human Molecular Genetics*, 8, (1999). doi: 10.1093/hmg/8.3.387.

[65] E. Korzus, M. G. Rosenfeld, and M. Mayford. CBP histone acetyltransferase activity is a critical component of memory consolidation. *Neuron*, 42, (2004). doi: 10.1016/j.neuron.2004.06.002.

[66] J.-S. Guan, S. J. Haggarty, E. Giacometti, J.-H. Dannenberg, N. Joseph, J. Gao, T. J. F. Nieland, Y. Zhou, X. Wang, R. Mazitschek, J. E. Bradner, R. A. DePinho, R. Jaenisch, and L.-H. Tsai. HDAC2 negatively regulates memory formation and synaptic plasticity. *Nature*, 459, (2009). doi: 10.1038/nature07925.

[67] G. Chen, X. Zou, H. Watanabe, J. M. van Deursen, and J. Shen. CREB binding protein is required for both short-term and long-term memory formation. *Journal of Neuroscience*, 30, (2010). doi: 10.1523/JNEUROSCI.2378-10.2010.

[68] S. A. Maddox, C. S. Watts, and G. E. Schafe. p300/CBP histone acetyltransferase activity is required for newly acquired and reactivated fear memories in the lateral amygdala. *Learning Memory*, 20, (2013). doi: 10.1101/lm.029157.112.

[69] C. H. Arrowsmith, C. Bountra, P. V. Fish, K. Lee, and M. Schapira. Epigenetic protein families: a new frontier for drug discovery. *Nature Reviews Drug Discovery*, 11:384–400, (2012). doi: 10.1038/nrd3674.

[70] T. Yamamoto and M. Horikoshi. Novel substrate specificity of the histone acetyltransferase activity of HIV-1-Tat interactive protein Tip60. *Journal of Biological Chemistry*, 272:30595–30598, (1997). doi: 10.1074/jbc.272.49.30595.

[71] I. Urban, C. Kerimoglu, M. S. Sakib, H. Wang, E. Benito, C. Thaller, X. Zhou, J. Yan, A. Fischer, and G. Eichele. TIP60/KAT5 is required for neuronal viability in hippocampal CA1. *Scientific Reports*, 9, (2019). doi: 10.1038/s41598-019-50927-1.

[72] J. Gräff, D. Rei, J.-S. Guan, W.-Y. Wang, J. Seo, K. M. Hennig, T. J. F. Nieland, D. M. Fass, P. F. Kao, M. Kahn, S. C. Su, A. Samiei, N. Joseph, S. J. Haggarty, I. Delalle, and L.-H. Tsai. An epigenetic blockade of cognitive functions in the neurodegenerating brain. *Nature*, 483, (2012). doi: 10.1038/nature10849.

[73] J. A. Hardy and G. A. Higgins. Alzheimer's disease: The amyloid cascade hypothesis. *Science*, 256:184–185, (1992). doi: 10.1126/science.1566067.

[74] S. K. Pirooznia, J. Sarthi, A. A. Johnson, M. S. Toth, K. Chiu, S. Koduri, and F. Elefant. Tip60 HAT activity mediates APP induced lethality and apoptotic cell death in the CNS of a Drosophila Alzheimer's disease model. *PLoS ONE*, 7:e41776, (2012). doi: 10.1371/journal.pone.0041776.

[75] C. Rouaux. Critical loss of CBP/p300 histone acetylase activity by caspase-6 during neurodegeneration. *The EMBO Journal*, 22:6537–6549, (2003). doi: 10.1093/emboj/cdg615.

[76] C. U. Lithner, P. N. Lacor, W.-Q. Zhao, T. Mustafiz, W. L. Klein, J. D. Sweatt, and C. M. Hernandez. Disruption of neocortical histone H3 homeostasis by soluble a: implications for Alzheimer's disease. *Neurobiology of Aging*, 34:2081–2090, (2013). doi: 10.1016/j.neurobiolaging.2012.12.028.

[77] K. B. J. Paxinos, G. Franklin. *Paxinos and Franklin's the Mouse Brain in Stereotaxic Coordinates*. Academic Press, (2001).

[78] S. M. Rodrigues. Pavlovian fear conditioning regulates Thr286 autophosphorylation of Ca^{2+}/calmodulin-dependent protein kinase II at lateral amygdala synapses. *Journal of Neuroscience*, 24:3281–3288, (2004). doi: 10.1523/JNEUROSCI.5303-03.2004.

[79] K. K. Lee and J. L. Workman. Histone acetyltransferase complexes: one size doesn't fit all. *Nature Reviews Molecular Cell Biology*, 8, (2007). doi: 10.1038/nrm2145.

[80] E. Calo and J. Wysocka. Modification of enhancer chromatin: What, how, and why? *Molecular Cell*, 49:825–837, (2013). doi: 10.1016/j.molcel.2013.01.038.

[81] Q. Jin, L.-R. Yu, L. Wang, Z. Zhang, L. H. Kasper, J.-E. Lee, C. Wang, P. K. Brindle, S. Y. R. Dent, and K. Ge. Distinct roles of GCN5/PCAF-mediated H3K9ac and CBP/p300-mediated H3K18/27ac in nuclear receptor transactivation. *The EMBO Journal*, 30:249–262, (2011). doi: 10.1038/emboj.2010.318.

[82] G. D. Gale. Role of the basolateral amygdala in the storage of fear memories across the adult lifetime of rats. *Journal of Neuroscience*, 24:3810–3815, (2004). doi: 10.1523/JNEUROSCI.4100-03.2004.

[83] U. Blömer, L. Naldini, T. Kafri, D. Trono, I. M. Verma, and F. H. Gage. Highly efficient and sustained gene transfer in adult neurons with a lentivirus vector. *Journal of Virology*, 71, (1997). doi: 10.1128/jvi.71.9.6641-6649.1997.

[84] P. Mews, G. Donahue, A. M. Drake, V. Luczak, T. Abel, and S. L. Berger. Acetyl-CoA synthetase regulates histone acetylation and hippocampal memory. *Nature*, 546:381–386, (2017). doi: 10.1038/nature22405.

[85] J. Gräff and L.-H. Tsai. Histone acetylation: molecular mnemonics on the chromatin. *Nature Reviews Neuroscience*, 14, (2013). doi: 10.1038/nrn3427.

[86] A. M. Burns and J. Gräff. Cognitive epigenetic priming: leveraging histone acetylation for memory amelioration. *Current Opinion in Neurobiology*, 67:75–84, (2021). doi: 10.1016/j.conb.2020.08.011.

[87] S. C. Odell, F. Taki, S. L. Klein, R. J. Chen, O. B. Levine, M. J. Skelly, A. Nabila, E. Brindley, J. G. Toth, F. Dündar, C. K. Sheridan, R. N. Fetcho, A. Alonso, C. Liston, D. A. Landau, K. E. Pleil, and M. Toth. Epigenomically bistable regions across neuron-specific genes govern neuron eligibility to a coding ensemble in the hippocampus. *Cell Reports*, 31:107789, (2020). doi: 10.1016/j.celrep.2020.107789.

Supplementary Figures

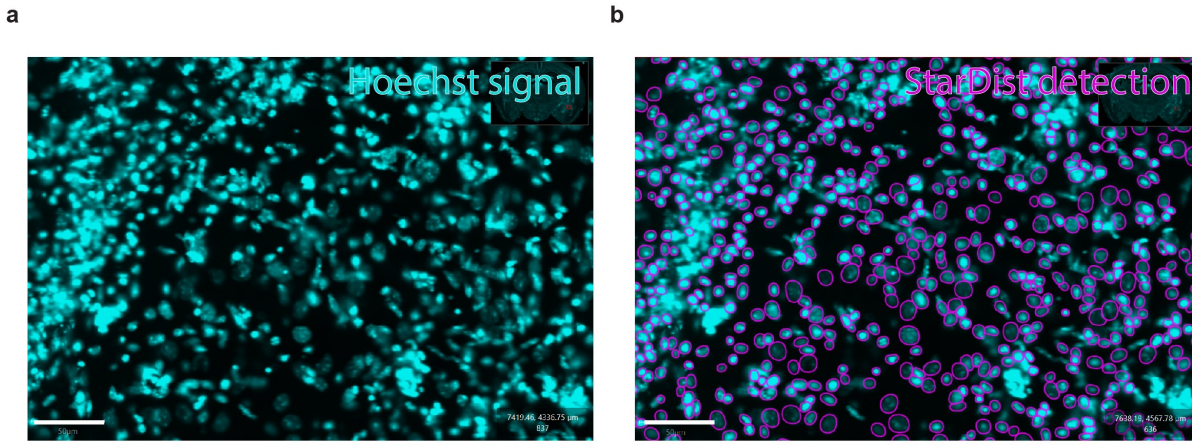

Supplementary Figure S.1: a Hoechst-based signal of neurons in a high inflammation region within the lateral amygdala. **b** Cell detection script optimized to detect cells that display normal morphology.

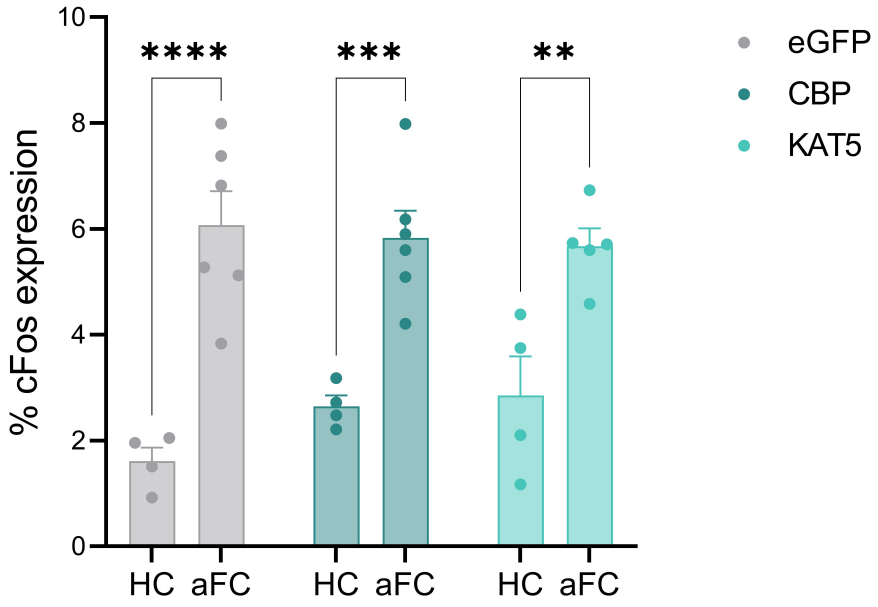

Supplementary Figure S.2: Quantification of cFos$^+$ neurons in the HC group (*n*= 12) compared to the aFC group (*n*= 17). Ordinary two-way ANOVA, *****P*= 0.0001, ***P*= 0.0009, **P*= 0.0041, Šídák's multiple comparison test. Data is represented as mean ± s.e.m. aFC, auditory fear conditioning; HC, home cage.

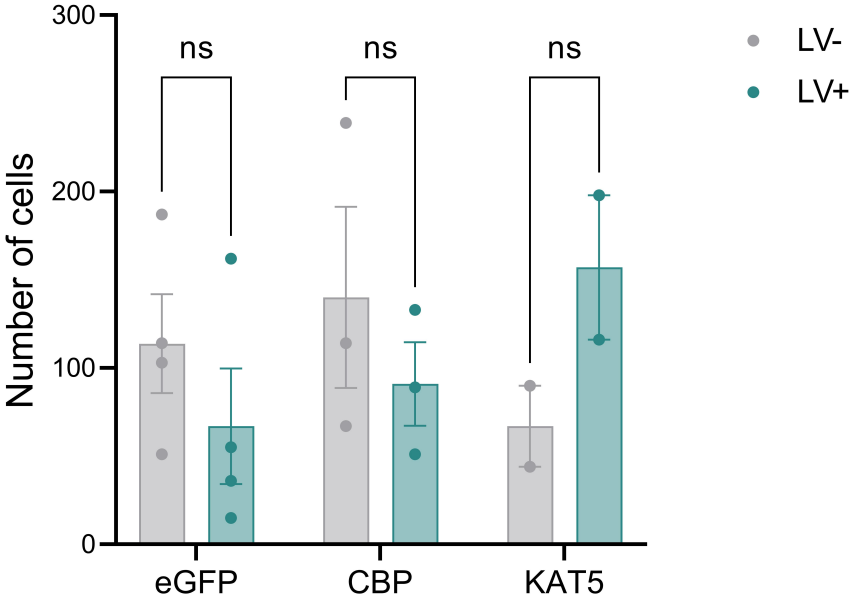

Supplementary Figure S.3: Cell count of LV^+ compared to LV^- in the HC group detected by the acetyl marker H3K27ac. Ordinary two-way ANOVA, Šídák's multiple comparison test. Data is represented as mean ± s.e.m. ns, not significant.

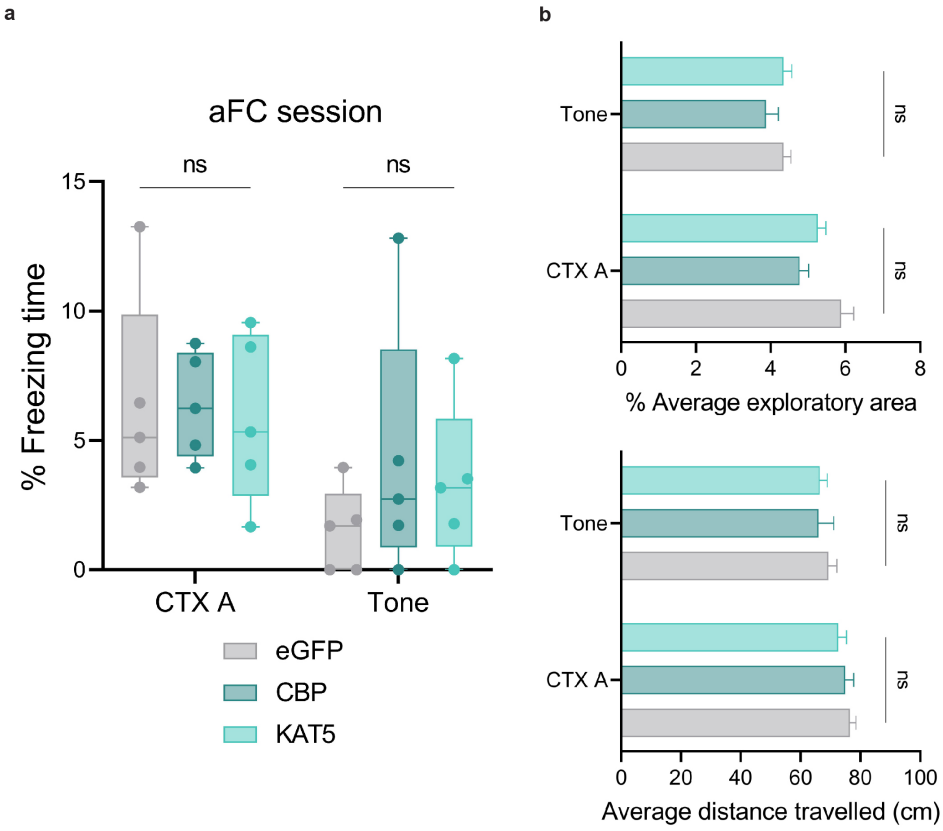

Supplementary Figure S.4: **a** Average percentage of freezing response during the 2 min habituation to the context (CTX) A and the 30 sec presentation of the auditory cue (Tone) in the recall group (*n*= 15). RM two-way ANOVA, Šídák's multiple comparison test. **b** Average percentage of exploratory area (top) and average distance travelled (bottom), during context A and Tone presentation in the aFC session. RM two-way ANOVA, Šídák's multiple comparison test. Data is represented as mean ± s.e.m. aFC, auditory fear conditioning; CTX, context; ns, not significant.

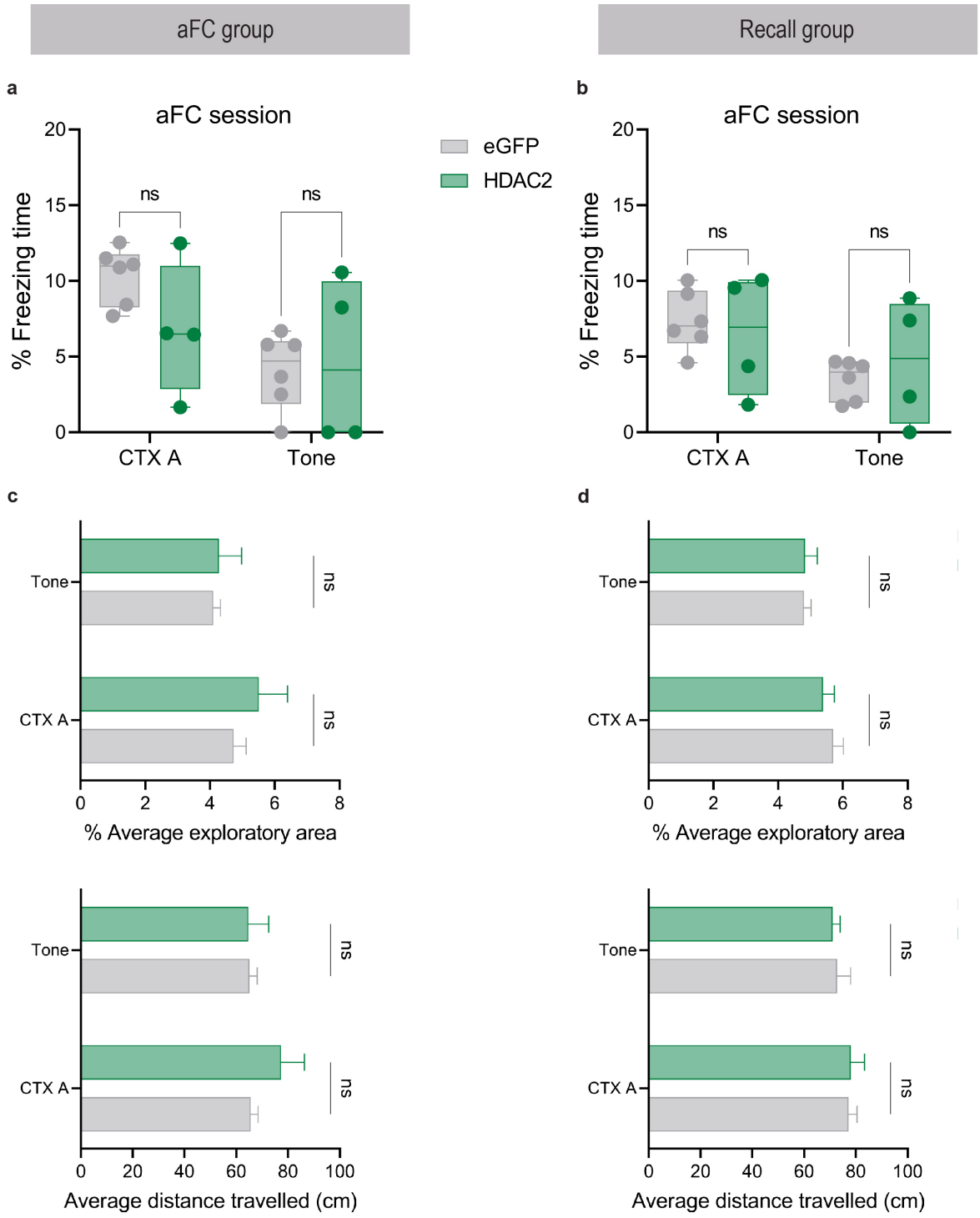

Supplementary Figure S.5: a Average percentage of freezing response during the 2 min habituation to the context (CTX) A and the 30 sec presentation of the auditory cue (Tone) in the aFC group (n= 10) and **b** the recall group (n= 10). RM two-way ANOVA, Šídák's multiple comparison test. **c** Average percentage of exploratory area (top) and average distance travelled (bottom), during context A and Tone presentation in the aFC group and **d** the recall group. RM two-way ANOVA, Šídák's multiple comparison test. Data is represented as mean ± s.e.m. aFC, auditory fear conditioning; CTX, context; ns, not significant.